Mathematical Biology

Final epidemic size of a two-community SIR model with asymmetric coupling

Zhimin Han[1] · Yi Wang[1] · Shan Gao[2,3] · Guiquan Sun[4] · Hao Wang[2,3]

© The Author(s), under exclusive licence to Springer-Verlag GmbH Germany, part of Springer Nature 2024

Abstract

Communities are commonly not isolated but interact asymmetrically with each other, allowing the propagation of infectious diseases within the same community and between different communities. To reveal the impact of asymmetrical interactions and contact heterogeneity on disease transmission, we formulate a two-community SIR epidemic model, in which each community has its contact structure while communication between communities occurs through temporary commuters. We derive an explicit formula for the basic reproduction number $\mathcal{R}_0$, give an implicit equation for the final epidemic size z, and analyze the relationship between them. Unlike the typical positive correlation between $\mathcal{R}_0$ and z in the classic SIR model, we find a negatively correlated relationship between counterparts of our model deviating from homogeneous populations. Moreover, we investigate the impact of asymmetric coupling mechanisms on $\mathcal{R}_0$. The results suggest that, in scenarios with restricted movement of susceptible individuals within a community, $\mathcal{R}_0$ does not follow a simple monotonous relationship, indicating that an unbending decrease in the movement of susceptible individuals may increase $\mathcal{R}_0$. We further demonstrate that network contacts within communities have a greater effect on $\mathcal{R}_0$ than casual contacts between communities. Finally, we develop an epidemic model without restriction on the movement of susceptible individuals, and the numerical simulations suggest that the increase in human flow between communities leads to a larger $\mathcal{R}_0$.

✉ Hao Wang
    hao8@ualberta.ca

[1] School of Mathematics and Physics, China University of Geosciences, Wuhan 430074, Hubei, China

[2] Department of Mathematical and Statistical Sciences, University of Alberta, Edmonton, AB T6G 2G1, Canada

[3] Interdisciplinary Lab for Mathematical Ecology and Epidemiology, University of Alberta, Edmonton, AB T6G 2G1, Canada

[4] School of Mathematics, North University of China, Taiyuan 030051, Shanxi, China

1 Introduction

The struggle between human beings and infectious diseases has never stopped. Historically, the plague pandemic in the middle ages was exceptionally severe, causing an estimated 25 million deaths in Europe, accounting for a quarter of the population of 100 million (Thieme 2003). Over the past two decades, people have experienced global health threats posed by infectious diseases, such as the SARS epidemic between 2002 and 2003, the influenza H1N1 outbreak in 2009, and the Ebola epidemic in West Africa between 2013 and 2016. For now, corona virus disease 2019 (COVID-19) is still ongoing and even more uncontrolled due to more frequent population movement. Infectious diseases have been an ever-present global concern in the public health field, causing significant economic losses and affecting human health every year. In order to prevent the occurrence of infectious diseases and mitigate their impact, it is particularly important to have a detailed understanding of the dynamics of the disease. Thus, mathematical modelling for infectious diseases at the population or community levels continues to receive much attention (Velazquez et al. 1990; Hales et al. 1999; Wallis and Lee 1999; El Sayed et al. 2000).

Previous research on epidemiological models is commonly based on the particular assumption of homogeneous mixing (Anderson and May 1992; Hethcote 2000), which means that each individual in the population has an equal contact probability, and infected individuals will have the same probability of infecting the susceptible population. The spread of an epidemic among a population depends on the proportion of contacts between individuals. For instance, individuals from a relatively large population can only contact with a limited part of the overall population, the standard mean-field model is then no longer applicable in such case. Therefore, it is more practical to consider populations that are heterogeneously mixed. Heterogeneous mixing of populations can be categorized in many ways, such as contact heterogeneity, spatial heterogeneity (Lajmanovich and Yorke 1976; Thieme 1977; Diekmann 1978; Rass and Radcliffe 2003; Muroya et al. 2013), etc. Thieme (1977) and Diekmann (1978) derived the final size equations for the space-dependent model. Rass and Radcliffe (2003) gave the final size equations for non-spatial and spatial multi-type models in sections 2.5 and 3.4 of their book, respectively. Fitzgibbon et al. (2019) investigated a time-dependent spatial vector-host epidemic model with non-coincident domains for the vector and host populations and established global well-posedness and uniform prior bounds as well as the long-term behavior. Subsequently, Fitzgibbon et al. (2020) developed a dynamic model of an evolving epidemic in a spatially inhomogeneous environment to predict disease outbreaks and spatio-temporal spread. They demonstrated the existence and uniform boundedness of the solutions and studied their long-term behavior. In addition, contact network models have appeared in the public view as an attempt to shape contact heterogeneity in populations. Research on

the dynamics of disease transmission on the network has been done in the past two decades (Pastor-Satorras and Vespignani 2001; Wang and Dai 2008; Jin et al. 2014; Wang et al. 2020).

On a connected network, each node and edge represent an individual and a possible connection between individuals, respectively. Individuals connected by the edge are named neighbours. Regular contact networks (each node in the network has exactly k links) can model the dynamics for certain populations, such as those initially caused by veterinary applications and spatially embedded ecology. However, regular contact networks may underperform for sexually transmitted diseases (Kamp 2010) and human respiratory transmitted diseases (Mossong et al. 2008), since their contact networks are highly heterogeneous. Therefore, it is more practical to consider heterogeneous contacts among individuals in the modelling process. Heterogeneous contact network models are employed extensively to study the dynamics of disease transmission. In 2002, Moreno et al. (2002) formulated a susceptible-infected-recovered (SIR) model in heterogeneous networks, which is based on the states of nodes and their degrees, and showed the effect of degree distribution on the epidemic threshold and the final outbreak size. Various epidemic models based on the idea of heterogeneous networks have been proposed and analyzed. Barthélemy et al. (2005) studied the prevalence thresholds of diseases and the dynamics of disease outbreaks over time in a population with complex and heterogeneous connection patterns. It was shown that in all networks with fluctuating degrees of dispersion, the prevalence increases rapidly and does not depend on the architecture of the connection correlation function describing the population network. Zhu et al. (2012) investigated the transmission dynamics of diseases in populations with complex heterogeneous network structures, and the results elucidated why heterogeneous connection structures affect disease prevalence thresholds and concluded that network heterogeneity drives disease transmission. Großmann et al. (2021) used a network of contacts to model the complex structure of interactions between individuals and proposed a role for contact heterogeneity in the COVID-19 pandemic. For more studies on the transmission of epidemics in heterogeneous contact networks refer to Olinky and Stone (2004), Graham and House (2014), Meng et al. (2021), Amini and Minca (2022).

The disease prevalence can only be reduced with human intervention but can hardly be eradicated. People are interested in whether a disease can invade a population and how the disease is affected by contact patterns, which motivates us to study the impact of contact patterns on the threshold and final epidemic size of the disease. Pastor-Satorras and Vespignani (2001) found that there is no epidemic threshold in scale-free networks with the divergence of the second moment for the degree distribution, contrary to scalar deterministic models. Kiss et al. (2006) studied the dynamics of disease transmission under multiple pathways of contact. They found that the final epidemic size of the disease increases with the mean field-type transmission contribution and decreases with the network transmission contribution. This indicates that the contact pattern has a strong influence on disease prevalence. Wang et al. (2018) established an edge-based SIR model of multi-path spread on a random network, calculated the basic reproduction number and type reproduction numbers, and derived the final epidemic size equations. In particular, the effect of degree distribution on the basic reproduction number and final size was analyzed.

Contact patterns in the population make a significant contribution to disease transmission. In particular, larger populations exhibit more diverse patterns of contact, owing to their inherently complex interaction both within and outside their respective communities. Therefore, it is imperative to develop a comprehensive understanding of the disease transmission dynamics within and between communities, to restore the transmission dynamics in larger populations. Much work has been conducted on such considerations. In 2000, Hethcote (2000) quantified the relationship between the basic reproduction number and the final size of a single community using a mathematical expression. Zhang and Jin (2012) investigated the network SEAIR model with community structure, and obtained the basic reproduction number and final size of the model. Koch et al. (2013) studied the effect of randomly removing edges and reducing the proportion of external edges within and between communities on the basic reproduction number and final size. Lieberthal et al. (2023) investigated the impact of community structure on the transmission of epidemics in human metapopulation networks and emphasized the significant influence of community structure on disease reproduction rates. However, few works consider the solvability of implicit equations for the final epidemic size and the relationship between the basic reproduction number and the final epidemic size. To our knowledge, Bidari et al. (2016) analyzed the solvability of implicit final size equations for the SIR pairwise and heterogeneous mean-field models. Magal et al. (2016) and (2018) studied the final size problem for two- and multi-group SIR epidemic models, respectively. Additionally, Magal et al. (2016) presented the result on the relationship between the basic reproduction number and the final size.

Despite these previous efforts, our focus extends to dynamic scenarios involving unequal interaction between different communities (asymmetric coupling) and individuals with varying number of contacts (contact heterogeneity), a topic that remains unclear. To address this, we formulate a two-community SIR epidemic model with asymmetric coupling. In addition to intra-community individual contacts, our model also incorporates inter-community individual contacts through travel activities (e.g., purchase, recreation, commute, etc) due to the inconsistency of the public preventative measures in each community, which leads to different probabilities of contact between individuals within and between communities. Based on the proposed high-dimensional two-community SIR model with asymmetric coupling, we derive the explicit expression for the basic reproduction number and the implicit equations for the final size, and prove the existence and uniqueness of the solution to the implicit equations. Furthermore, we analyze the relationship between the basic reproduction number and the final size.

This paper is organized into the following sections. In Sect. 2, we develop a two-community SIR model with asymmetric coupling, in which each community is described by a heterogeneous network. In Sect. 3, we derive the basic reproduction number and final size of the model, and prove the existence and uniqueness of the solution of implicit equations for the final size. Furthermore, to obtain the explicit expression of the basic reproduction number, we reformulate the original model using an edge-based compartmental modelling approach. In Sect. 4, sensitivity analysis and numerical simulations are given to demonstrate the impact of the degree distribution and asymmetric coupling mechanism on the basic reproduction number and final epi-

demic size. We conclude the paper with the limitations of the current study and list some future directions in Sect. 5.

2 Model description

In this paper, we consider the disease transmission between two communities without birth and death. Here, we assume that an infected individual in one community can visit another community by shopping, going to work, visiting, etc., resulting in the susceptible population of visiting community being infected. When studying the epidemic transmission on a network, individuals are considered as nodes, while contacts among individuals are considered as edges. To solve the heterogeneity of contacts among individuals, the population of community A is divided into n_A different groups N_k^A ($k = 1, 2, \ldots, n_A$), and each individual in group k is in contact with exactly k individuals; here, n_A is the maximum degree of community A. The population of community B is divided into n_B different groups N_l^B ($l = 1, 2, \ldots, n_B$), and each individual in group l is in contact with exactly l individuals; here, n_B is the maximum degree of community B. Community A population size is $N^A = N_1^A + N_2^A + \cdots + N_{n_A}^A$, then the probability of having the number of k contacts is $p^A(k) = N_k^A/N^A$. Community B population size is $N^B = N_1^B + N_2^B + \cdots + N_{n_B}^B$, then the probability of having the number of l contacts is $p^B(l) = N_l^B/N^B$. The model expresses the dynamics of disease transmission within a community and between communities (See Fig. 1). Define $S_k^A(t)$, $I_k^A(t)$ and $R_k^A(t)$ as the number of susceptible individuals, infected individuals and recovered individuals with a degree k at time t in community A, respectively. $S_l^B(t)$, $I_l^B(t)$ and $R_l^B(t)$ are counterparts but with degree l in community B. The total number of individuals in community A with degree k is $S_k^A(t) + I_k^A(t) + R_k^A(t) = N_k^A(t)$, and the total number of individuals in community B with degree l is $S_l^B(t) + I_l^B(t) + R_l^B(t) = N_l^B(t)$. For a susceptible individual of degree k, it becomes infected in two ways, through network contact with an infected individual in the same community or through casual contact with an infected individual in another community. The model is expressed in the form of the following system of ordinary differential equations with $3(n_A + n_B)$ variables

$$
\begin{cases}
\dot{S_k^A}(t) = -\tau_A \alpha k S_k^A \Theta_i^A - (1-\alpha)\sigma_A S_k^A \dfrac{I^B}{N^B}, \\[2mm]
\dot{I_k^A}(t) = \tau_A \alpha k S_k^A \Theta_i^A + (1-\alpha)\sigma_A S_k^A \dfrac{I^B}{N^B} - \gamma_A I_k^A, \\[2mm]
\dot{R_k^A}(t) = \gamma_A I_k^A, \\[2mm]
\dot{S_l^B}(t) = -\tau_B \beta l S_l^B \Theta_i^B - (1-\beta)\sigma_B S_l^B \dfrac{I^A}{N^A}, \\[2mm]
\dot{I_l^B}(t) = \tau_B \beta l S_l^B \Theta_i^B + (1-\beta)\sigma_B S_l^B \dfrac{I^A}{N^A} - \gamma_B I_l^B, \\[2mm]
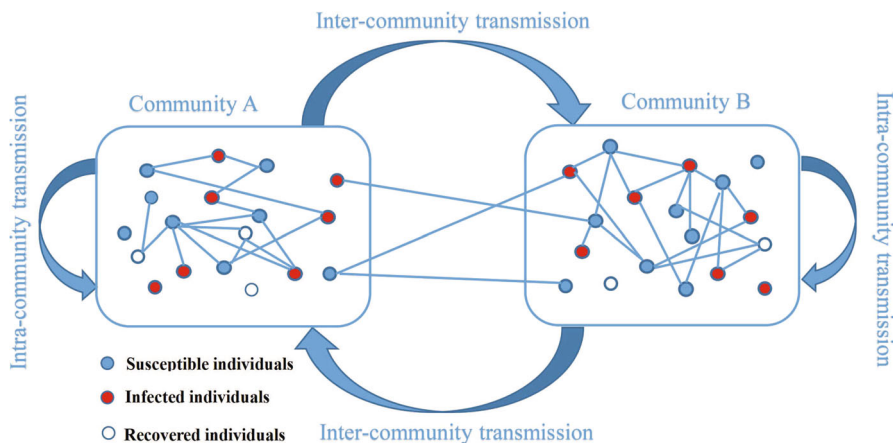\dot{R_l^B}(t) = \gamma_B I_l^B,
\end{cases}
\tag{2.1}
$$

Fig. 1 Flow diagram of the two-community network SIR model with asymmetric coupling (Color figure online)

Table 1 Description of the model (2.1) parameters

Parameters	Description
$\tau_A > 0$	Transmission probability from an infectious individual to a susceptible individual in the community A through network contact
$\tau_B > 0$	Transmission probability from an infectious individual to a susceptible individual in the community B through network contact
$\sigma_A > 0$	Transmission probability from an infectious individual in the community B to a susceptible individual in the community A through casual contact
$\sigma_B > 0$	Transmission probability from an infectious individual in the community A to a susceptible individual in the community B through casual contact
$0 \leq \alpha \leq 1$	The contribution of disease transmission through intra-community A
$1 - \alpha$	The contribution of disease transmission from community B to community A
$0 \leq \beta \leq 1$	The contribution of disease transmission through intra-community B
$1 - \beta$	The contribution of disease transmission from community A to community B
$\gamma_A > 0$	The recovery rate of infected individuals in community A
$\gamma_B > 0$	The recovery rate of infected individuals in community B

where $I^A(t) = \sum_{j=1}^{n_A} I_j^A(t)$, $I^B(t) = \sum_{j=1}^{n_B} I_j^B(t)$. The term $\Theta_i^A(t) = \frac{\sum_{j=1}^{n_A} j I_j^A(t)}{\sum_{j=1}^{n_A} j N_j^A(t)}$ is the expectation that any given edge on the connected network of community A points to an infected node in the same community, and $\Theta_i^B(t) = \frac{\sum_{j=1}^{n_B} j I_j^B(t)}{\sum_{j=1}^{n_B} j N_j^B(t)}$ is the expectation that any given edge on the connected network of community B points to an infected node in the same community. In real life, individuals who are infected with an epidemic generally need to rest and do not engage in travel activities. To account for this, we introduce the parameter α to represent the movement restriction of susceptible

individuals in the community A. Specifically, when $\alpha = 1$, it means that susceptible individuals in community A are restricted from moving; when $\alpha = 0$, susceptible individuals have unrestricted movement. For $0 < \alpha < 1$, a fraction of susceptible individuals are allowed to leave the community. In addition, we can explain it from the perspective of what leads to the spread of disease in a community. We categorize the susceptible individuals in community A to contract the disease into two pathways: αS_k^A of the susceptible individuals are infected through contact with infected individuals within community A, while $(1 - \alpha)S_k^A$ of the susceptible individuals are infected through contact with infected individuals in community B. A similar interpretation applies to the parameter β regarding to community B. Additional parameters in this model are described in Table 1.

Dividing the first $3n_A$ equations of the model (2.1) by $N_k^A(t)$ and the last $3n_B$ equations by $N_l^B(t)$ gives

$$
\begin{cases}
\dot{s}_k^A(t) = -\tau_A \alpha k s_k^A \Theta_i^A - (1 - \alpha)\sigma_A s_k^A i^B, \\
\dot{i}_k^A(t) = \tau_A \alpha k s_k^A \Theta_i^A + (1 - \alpha)\sigma_A s_k^A i^B - \gamma_A i_k^A, \\
\dot{r}_k^A(t) = \gamma_A i_k^A, \\
\dot{s}_l^B(t) = -\tau_B \beta l s_l^B \Theta_i^B - (1 - \beta)\sigma_B s_l^B i^A, \\
\dot{i}_l^B(t) = \tau_B \beta l s_l^B \Theta_i^B + (1 - \beta)\sigma_B s_l^B i^A - \gamma_B i_l^B, \\
\dot{r}_l^B(t) = \gamma_B i_l^B,
\end{cases}
\tag{2.2}
$$

where $\Theta_i^A(t) = \sum_{j=1}^{n_A} \frac{j p^A(j)}{\langle k \rangle_A} i_j^A(t)$, $\Theta_i^B(t) = \sum_{j=1}^{n_B} \frac{j p^B(j)}{\langle k \rangle_B} i_j^B(t)$, $i^A(t) = \sum_{j=1}^{n_A} p^A(j) i_j^A(t)$, and $i^B(t) = \sum_{j=1}^{n_B} p^B(j) i_j^B(t)$; $p^A(j) = \frac{N_j^A}{N^A}$ is the degree distribution of the community A, $p^B(j) = \frac{N_j^B}{N^B}$ is the degree distribution of the community B, $\langle k \rangle_A = \sum_{j=1}^{n_A} j p^A(j)$ is the mean degree of community A, $\langle k \rangle_B = \sum_{j=1}^{n_B} j p^B(j)$ is the mean degree of community B. Moreover, $s_k^A(t) = \frac{S_k^A(t)}{N_k^A(t)}, i_k^A(t) = \frac{I_k^A(t)}{N_k^A(t)}, r_k^A(t) = \frac{R_k^A(t)}{N_k^A(t)}$ denote the relative density of susceptible, infected and recovered individuals with degree k at time t in community A, respectively, and $s_l^B(t) = \frac{S_l^B(t)}{N_l^B(t)}, i_l^B(t) = \frac{I_l^B(t)}{N_l^B(t)}$, $r_l^B(t) = \frac{R_l^B(t)}{N_l^B(t)}$ denote the relative density of susceptible, infected and recovered individuals with degree l at time t in community B, respectively. The initial values of model (2.2) are $s_k^A(0) = 1 - \varepsilon_k^A$, $s_l^B(0) = 1 - \varepsilon_l^B$, $i_k^A(0) = \varepsilon_k^A$, $i_l^B(0) = \varepsilon_l^B$ with $0 \leq \varepsilon_k^A, \varepsilon_l^B \ll 1$, $r_k^A(0) = 0$, and $r_l^B(0) = 0$.

For spatially discretely distributed multi-patch models, it is usually assumed that individuals in each patch are homogeneously mxied. For epidemic dynamics in annealed networks, individuals are classified also by their degrees k, that is, individuals with the same degree are considered statistically equivalent. Mathematically, there may not be much difference from multi-patch or multi-group epidemic models, but the results from theoretical analysis can vary. For example, the global problem of

endemic equilibrium in the multi-group SIRS epidemic model remains incompletely solved, while that of the network SIRS model has been completely solved. Muroya et al. (2013) and Muroya and Kuniya (2014) found that the global stability of endemic equilibrium in the multi-group SIRS epidemic model requires further conditions in addition to the basic reproduction number $R_0 > 1$. Li et al. (2014) proposed an SIRS model on a complex network and derived that the endemic equilibrium is globally asymptotically stable when $R_0 > 1$. Motivated by these facts, the network epidemic model may yield new results and provide new insights.

3 Main results

The goal of this section is to study the dynamics of the given model. We mathematically investigate the positivity of solutions, the explicit expression of basic reproduction number, as well as the implicit equations of final epidemic size.

3.1 Positivity of solutions

The positivity of the solution of model (2.2) is demonstrated by the following. In previous studies, the differential equation for the relative density of recovered individuals is often ignored, but here we omit the differential equation for susceptible individuals from model (2.2). Let $\vec{Y}(t) = \left(i_1^A(t), i_2^A(t), \cdots, i_{n_A}^A(t), r_1^A(t), r_2^A(t), \ldots, r_{n_A}^A(t), i_1^B(t), i_2^B(t), \ldots, i_{n_B}^B(t), r_1^B(t), r_2^B(t), \cdots, r_{n_B}^B(t)\right)$, $Y_i \in [0, 1]$, $i = 1, \ldots, 2(n_A + n_B)$, $Y_k = i_k^A(t)$, $Y_{k+n_A} = r_k^A(t)$, $k = 1, \ldots, n_A$, $Y_{l+2n_A} = i_l^B(t)$, $Y_{l+2n_A+n_B} = r_l^B(t)$, $l = 1, \ldots, n_B$.

Theorem 3.1 *If $\vec{Y}(0) \in \Lambda_{2(n_A+n_B)} = \Pi_{i=1}^{2(n_A+n_B)}[0, 1]$, then $\vec{Y}(t) \in \Lambda_{2(n_A+n_B)}$ for any $t > 0$.*

Proof In fact, proving this is equivalent to proving that $\Lambda_{2(n_A+n_B)}$ is a positive invariant set of model (2.2). Define

$$\partial \Lambda_{2(n_A+n_B)}^1 = \{\vec{Y}(t) \in \Lambda_{2(n_A+n_B)} \mid Y_i = 0 \text{ for some } i\},$$
$$\partial \Lambda_{2(n_A+n_B)}^2 = \{\vec{Y}(t) \in \Lambda_{2(n_A+n_B)} \mid Y_i = 1 \text{ for some } i\},$$

where $i = 1, \ldots, 2(n_A + n_B)$ and $\partial \Lambda$ is the boundary of Λ. Define the outer normal as $\xi_i^1 = (\overbrace{0, \ldots, -1}^{i}, \ldots, 0)$ and $\xi_i^2 = -\xi_i^1$. Yorke (1967) has proved that for any compact set Ω which is invariant for $\dot{x} = f(x)$, the vector $f(x)$ is zero or points to the set for any point x in $\partial \Omega$. We use the method in Yorke (1967) to prove that $\Lambda_{2(n_A+n_B)}$

is an invariant set of model (2.2). From Eq. (2.2), one has

$$
\begin{cases}
\left(\frac{d\vec{Y}}{dt}\big|_{Y_i=0} \cdot \xi_i^1\right) = -(1 - Y_{i+n_A}(t))\left[\frac{\tau_A \alpha i}{\langle k \rangle_A} \sum_{j \neq i}^{n_A} j p^A(j) Y_j(t)\right. \\
\qquad\qquad\qquad\qquad\qquad \left. + (1-\alpha)\sigma_A \sum_{j \neq i}^{n_B} p^B(j) Y_{j+2n_A}(t)\right] \\
\qquad \leq 0, \text{ for } i = 1, \ldots, n_A, \\
\left(\frac{d\vec{Y}}{dt}\big|_{Y_i=0} \cdot \xi_i^1\right) = -\gamma_A \cdot Y_{i-n_A}(t) \leq 0, \text{ for } i = n_A + 1, \ldots, 2n_A, \\
\left(\frac{d\vec{Y}}{dt}\big|_{Y_i=0} \cdot \xi_i^1\right) = -(1 - Y_{i+n_B}(t))\left[\frac{\tau_B \beta i}{\langle k \rangle_B} \sum_{j \neq i}^{n_B} j p^B(j) Y_{j+2n_A}(t)\right. \\
\qquad\qquad\qquad\qquad\qquad \left. + (1-\beta)\sigma_B \sum_{j \neq i}^{n_A} p^A(j) Y_j(t)\right] \\
\qquad \leq 0, \text{ for } i = 2n_A + 1, \ldots, 2n_A + n_B, \\
\left(\frac{d\vec{Y}}{dt}\big|_{Y_i=0} \cdot \xi_i^1\right) = -\gamma_B \cdot Y_{i-n_B}(t) \leq 0, \text{ for } i = 2n_A + n_B + 1, \ldots, 2n_A + 2n_B.
\end{cases}
$$

And it is easy to derive $\frac{d\vec{Y}}{dt}\big|_{Y_i=1} \cdot \xi_i^2 \leq 0, i = 1, \ldots, 2n_A + 2n_B$. Hence, an arbitrary solution starting in $\partial\Lambda^1_{2(n_A+n_B)} \bigcup \partial\Lambda^2_{2(n_A+n_B)}$ remains in $\Lambda_{2(n_A+n_B)}$, such that $\Lambda_{2(n_A+n_B)}$ is a positive invariant set of model (2.2). ∎

3.2 Basic reproduction number

We conclude that the disease-free equilibrium of system (2.2) is $E_0 = (\underbrace{1, 1, \ldots, 1,}_{n_A}$
$\underbrace{0, 0, \ldots, 0,}_{2n_A} \underbrace{1, 1, \ldots, 1,}_{n_B} \underbrace{0, 0, \ldots, 0}_{2n_B})$. In epidemiology, the basic reproduction number is defined as the expected number of secondary infections through a single infected individual in a population of all susceptible individuals. In the following, we use the next-generation matrix method from literature (Van den Driessche and Watmough 2002) to calculate the basic reproduction number of the model. In model (2.2), the rate of appearance of new infections and the rate of transfer of individuals out of the compartments satisfy (A1)-(A5) in Van den Driessche and Watmough (2002). When the system is in a disease-free state, we obtain the new infection matrix and transition matrix as follows:

$$
\mathcal{F}_{(n_A+n_B)\times(n_A+n_B)} = \begin{bmatrix} F_{11} & F_{12} \\ F_{21} & F_{22} \end{bmatrix}, \mathcal{V}_{(n_A+n_B)\times(n_A+n_B)} = \begin{bmatrix} V_1 & 0 \\ 0 & V_2 \end{bmatrix},
$$

where the block matrix $F_{11} = \frac{\tau_A \alpha}{\langle k \rangle_A} \begin{bmatrix} 1 \\ 2 \\ \vdots \\ n_A \end{bmatrix} \left[1 p^A(1), 2 p^A(2), \ldots, n_A p^A(n_A) \right]$, $F_{12} =$

$(1-\alpha)\sigma_A \begin{bmatrix} 1 \\ 1 \\ \vdots \\ 1 \end{bmatrix} \left[p^B(1), p^B(2), \ldots, p^B(n_B) \right]$, $F_{21} = (1-\beta)\sigma_B \begin{bmatrix} 1 \\ 1 \\ \vdots \\ 1 \end{bmatrix} [p^A(1), p^A(2),$

$\ldots, p^A(n_A)]$, $F_{22} = \frac{\tau_B \beta}{\langle k \rangle_B} \begin{bmatrix} 1 \\ 2 \\ \vdots \\ n_B \end{bmatrix} \left[1 p^B(1), 2 p^B(2), \ldots, n_B p^B(n_B) \right]$, $V_1 = diag(\gamma_A, \gamma_A,$

$\ldots, \gamma_A)$ and $V_2 = diag(\gamma_B, \gamma_B, \ldots, \gamma_B)$.

By calculation, we get

$$\mathcal{V}^{-1}_{(n_A+n_B) \times (n_A+n_B)} = \begin{bmatrix} V_1^{-1} & 0 \\ 0 & V_2^{-1} \end{bmatrix},$$

where $V_1^{-1} = diag(\frac{1}{\gamma_A}, \frac{1}{\gamma_A}, \ldots, \frac{1}{\gamma_A})$ and $V_2^{-1} = diag(\frac{1}{\gamma_B}, \frac{1}{\gamma_B}, \ldots, \frac{1}{\gamma_B})$.

The basic reproduction number is the spectral radius of the next generation matrix $\mathcal{F}\mathcal{V}^{-1}$, that is,

$$\mathcal{R}_0 = \rho(\mathcal{F}\mathcal{V}^{-1}).$$

From the above analysis we know that the dimensionality of matrix $\mathcal{F}\mathcal{V}^{-1}$ is relatively high, we give the explicit expression for the basic reproduction number later by the idea of dimensionality reduction. Here, we first present the basic reproduction numbers for some special cases.

1. $\alpha = 1, 0 < \beta \leq 1$. $\alpha = 1$ means that susceptible individuals in community A are restricted from moving. The new infection matrix and transition matrix become

$$\mathcal{F}_{(n_A+n_B) \times (n_A+n_B)} = \begin{bmatrix} F_{11} & 0 \\ F_{21} & F_{22} \end{bmatrix}, \mathcal{V}_{(n_A+n_B) \times (n_A+n_B)} = \begin{bmatrix} V_1 & 0 \\ 0 & V_2 \end{bmatrix},$$

where the block matrix $F_{11} = \frac{\tau_A}{\langle k \rangle_A} \begin{bmatrix} 1 \\ 2 \\ \vdots \\ n_A \end{bmatrix} \left[1 p^A(1), 2 p^A(2), \ldots, n_A p^A(n_A) \right]$.

The block matrices F_{21}, F_{22}, V_1 and V_2 have the same form above. Then the next generation matrix is $\mathcal{F}\mathcal{V}^{-1} = \begin{bmatrix} F_{11} V_1^{-1} & 0 \\ F_{21} V_1^{-1} & F_{22} V_2^{-1} \end{bmatrix}$. Thus, we obtain the basic reproduction number

$$\mathcal{R}_0 = \rho(\mathcal{F}\mathcal{V}^{-1}) = \frac{1}{2}\left(\rho_{lA}\big|_{\alpha=1} + \rho_{lB}\right) + \frac{1}{2}\left[\left(\rho_{lA}\big|_{\alpha=1} + \rho_{lB}\right)^2 - 4\left(\rho_{lA}\big|_{\alpha=1}\right)\rho_{lB}\right]^{\frac{1}{2}}$$

$$= \max\left\{\rho_{lA}\big|_{\alpha=1}, \rho_{lB}\right\},$$

(3.1)

where $\rho_{lA} = \frac{\tau_A \alpha \langle k^2 \rangle_A}{\gamma_A \langle k \rangle_A}$ and $\rho_{lB} = \frac{\tau_B \beta \langle k^2 \rangle_B}{\gamma_B \langle k \rangle_B}$ are the basic reproduction numbers of diseases within communities A and B after the decoupling of the two-community disease transmission model, respectively. Specifically, when the two-community disease transmission model is decoupled, we obtain the spectral radius of matrix $\mathcal{F}\mathcal{V}^{-1}$ is only related to block matrices $F_{11}V_1^{-1}$ and $F_{22}V_2^{-1}$. This suggests that in the absence of disease transmission from community B to community A, the basic reproduction number $\mathcal{R}_0$ is determined by the greater one corresponding to the diseases within communities A and B. When $\beta = 1, 0 < \alpha \leq 1$, similar to the case of $\alpha = 1, 0 < \beta \leq 1$, it can be deduced that $\mathcal{R}_0 = \max\{\rho_{lA}, \rho_{lB}\big|_{\beta=1}\}$. In particular, when $\alpha = 1$, $\beta = 1$, the basic reproduction number is $\mathcal{R}_0 = \max\{\frac{\tau_A \langle k^2 \rangle_A}{\gamma_A \langle k \rangle_A}, \frac{\tau_B \langle k^2 \rangle_B}{\gamma_B \langle k \rangle_B}\}$.

2. $\alpha = 0, \beta = 0$. When $\alpha = 0, \beta = 0$, the next generation matrix is $\mathcal{F}\mathcal{V}^{-1} = \begin{bmatrix} 0 & F_{12}V_2^{-1} \\ F_{21}V_1^{-1} & 0 \end{bmatrix}$. A similar transformation of the next-generation matrix shows

that $\mathcal{F}\mathcal{V}^{-1}$ has the same eigenvalues as matrix $D = \begin{bmatrix} 0 & D_{12} \\ D_{21} & 0 \end{bmatrix}$, where $D_{12} =$

$\frac{\sigma_A}{\gamma_B} \begin{bmatrix} 1 \\ 0 \\ \vdots \\ 0 \end{bmatrix} \left[1, p^B(2), \ldots, p^B(n_B)\right]$, $D_{21} = \frac{\sigma_B}{\gamma_A} \begin{bmatrix} 1 \\ 0 \\ \vdots \\ 0 \end{bmatrix} \left[1, p^A(2), \ldots, p^A(n_A)\right]$, so

$\mathcal{R}_0 = \sqrt{\frac{\sigma_A \sigma_B}{\gamma_B \gamma_A}}$. This is the basic reproduction number when the disease does not spread within the same community, but only between two communities.

From Case 1, we learn that when the dynamics of disease development in one community are not influenced by the other, the basic reproduction number of the disease is determined by the greater one corresponding to the diseases within communities A and B. From Case 2, we know that when the disease spreads only between communities, the basic reproduction number is $\mathcal{R}_0 = \sqrt{\frac{\sigma_A \sigma_B}{\gamma_B \gamma_A}}$.

We now consider the explicit formula of the basic reproduction number for model (2.2). To this end, we borrow the idea from an edge-based compartmental approach (Miller et al. 2012). In the following, we give the exact derivation procedure by means of a low-dimensional system. From the first and fourth equations of model (2.2), one has

$$\ln \frac{s_k^A(t)}{s_k^A(0)} = -\sum_{j=1}^{n_A} \frac{kjp^A(j)}{\langle k \rangle_A} \int_0^t \tau_A \alpha i_j^A(s)ds - \sum_{j=1}^{n_B} p^B(j) \int_0^t (1-\alpha)\sigma_A i_j^B(s)ds,$$

$$\ln \frac{s_l^B(t)}{s_l^B(0)} = -\sum_{j=1}^{n_B} \frac{ljp^B(j)}{\langle k \rangle_B} \int_0^t \tau_B \beta i_j^B(s)ds - \sum_{j=1}^{n_A} p^A(j) \int_0^t (1-\beta)\sigma_B i_j^A(s)ds.$$

The above equations are equivalent to

$$
\begin{aligned}
s_k^A(t) &= (1-\varepsilon_k^A)e^{-\sum_{j=1}^{n_A} \frac{kjp^A(j)}{\langle k \rangle_A} \int_0^t \tau_A \alpha i_j^A(s)ds - \sum_{j=1}^{n_B} p^B(j) \int_0^t (1-\alpha)\sigma_A i_j^B(s)ds} \\
&= (1-\varepsilon_k^A)e^{-\sum_{j=1}^{n_A} \frac{kjp^A(j)}{\langle k \rangle_A} \int_0^t \tau_A \alpha i_j^A(s)ds} \cdot e^{-\sum_{j=1}^{n_B} p^B(j) \int_0^t (1-\alpha)\sigma_A i_j^B(s)ds} \\
&= (1-\varepsilon_k^A)(\theta_A)^k \Psi_A, \\
s_l^B(t) &= (1-\varepsilon_l^B)e^{-\sum_{j=1}^{n_B} \frac{ljp^B(j)}{\langle k \rangle_B} \int_0^t \tau_B \beta i_j^B(s)ds - \sum_{j=1}^{n_A} p^A(j) \int_0^t (1-\beta)\sigma_B i_j^A(s)ds} \\
&= (1-\varepsilon_l^B)e^{-\sum_{j=1}^{n_B} \frac{ljp^B(j)}{\langle k \rangle_B} \int_0^t \tau_B \beta i_j^B(s)ds} \cdot e^{-\sum_{j=1}^{n_A} p^A(j) \int_0^t (1-\beta)\sigma_B i_j^A(s)ds} \\
&= (1-\varepsilon_l^B)(\theta_B)^l \Psi_B,
\end{aligned}
\tag{3.2}
$$

where $\theta_A(t) = e^{-\sum_{j=1}^{n_A} \frac{jp^A(j)}{\langle k \rangle_A} \int_0^t \tau_A \alpha i_j^A(s)ds}$ represents the probability that a randomly selected stub has not spread the infection in community A, and $\Psi_A(t) = e^{-\sum_{j=1}^{n_B} p^B(j) \int_0^t (1-\alpha)\sigma_A i_j^B(s)ds} = e^{-(1-\alpha)\sigma_A \int_0^t i^B(s)ds}$ can be expressed as the probability of escaping the infection through casual contacts with community B. The meanings of $\theta_B(t) = e^{-\sum_{j=1}^{n_B} \frac{jp^B(j)}{\langle k \rangle_B} \int_0^t \tau_B \beta i_j^B(s)ds}$ and $\Psi_B(t) = e^{-\sum_{j=1}^{n_A} p^A(j) \int_0^t (1-\beta)\sigma_B i_j^A(s)ds} = e^{-(1-\beta)\sigma_B \int_0^t i^A(s)ds}$ are similar to that of $\theta_A(t)$ and $\Psi_A(t)$, respectively.

Thus, we obtain

$$
\begin{aligned}
s^A(t) &= \sum_{k=1}^{n_A} p^A(k)s_k^A = \sum_{k=1}^{n_A} (1-\varepsilon_k^A)p^A(k)(\theta_A)^k \Psi_A, \\
s^B(t) &= \sum_{l=1}^{n_B} p^B(l)s_l^B = \sum_{l=1}^{n_B} (1-\varepsilon_l^B)p^B(l)(\theta_B)^l \Psi_B.
\end{aligned}
\tag{3.3}
$$

Neglecting the degree correlation, the probability of randomly selected stubs connecting to nodes with a given state is equal to the proportion of all stubs associated with nodes with that state. Therefore, we need to consider below the proportions of stubs associated with susceptible, infected, and recovered nodes, which denote as $\Theta_s^A(t)$, $\Theta_i^A(t)$, and $\Theta_r^A(t)$ in community A and $\Theta_s^B(t)$, $\Theta_i^B(t)$, and $\Theta_r^B(t)$ in community B, respectively.

By the definitions of $\theta_A(t)$, $\Psi_A(t)$, $\theta_B(t)$, and $\Psi_B(t)$, we have

$$
\begin{aligned}
\theta_A'(t) &= -\tau_A \alpha \theta_A \Theta_i^A, \quad \Psi_A'(t) = -(1-\alpha)\sigma_A \Psi_A i^B, \\
\theta_B'(t) &= -\tau_B \beta \theta_B \Theta_i^B, \quad \Psi_B'(t) = -(1-\beta)\sigma_B \Psi_B i^A.
\end{aligned}
\tag{3.4}
$$

Since $\Theta_i^{A'}(t) = -\Theta_s^{A'}(t) - \gamma_A \Theta_i^A(t)$ and $\Theta_i^{B'}(t) = -\Theta_s^{B'}(t) - \gamma_B \Theta_i^B(t)$, we have to calculate $\Theta_s^A(t)$ and $\Theta_s^B(t)$. According to the meanings of $\Theta_s^A(t)$ and $\Theta_s^B(t)$, we write them as

$$\Theta_s^A(t) = \sum_{k=1}^{n_A} \frac{k p^A(k)}{\langle k \rangle_A} (1 - \varepsilon_k^A)(\theta_A)^k \Psi_A, \quad \Theta_s^B(t) = \sum_{l=1}^{n_B} \frac{l p^B(l)}{\langle k \rangle_B} (1 - \varepsilon_l^B)(\theta_B)^l \Psi_B,$$

where $\frac{k p^A(k)}{\langle k \rangle_A}$ and $\frac{l p^B(l)}{\langle k \rangle_B}$ are the probabilities that a stub belongs to a node with degree k in community A and a node with degree l in community B, respectively. In addition, $(1 - \varepsilon_k^A)(\theta_A(t))^k \Psi_A(t)$ and $(1 - \varepsilon_l^B)(\theta_B(t))^l \Psi_B(t)$ denote the probabilities that a node with degree k in community A and a node with degree l in community B are still susceptible nodes at time t, respectively.

Therefore, we have

$$
\begin{aligned}
\Theta_s^{A'}(t) = &-\tau_A \alpha \Theta_i^A \sum_{k=1}^{n_A} \frac{k^2 p^A(k)}{\langle k \rangle_A} (1 - \varepsilon_k^A)(\theta_A)^k \Psi_A \\
&- (1 - \alpha)\sigma_A \sum_{k=1}^{n_A} \frac{k p^A(k)}{\langle k \rangle_A} (1 - \varepsilon_k^A)(\theta_A)^k \Psi_A i^B, \\
\Theta_s^{B'}(t) = &-\tau_B \beta \Theta_i^B \sum_{l=1}^{n_B} \frac{l^2 p^B(l)}{\langle k \rangle_B} (1 - \varepsilon_l^B)(\theta_B)^l \Psi_B \\
&- (1 - \beta)\sigma_B \sum_{l=1}^{n_B} \frac{l p^B(l)}{\langle k \rangle_B} (1 - \varepsilon_l^B)(\theta_B)^l \Psi_B i^A.
\end{aligned}
\tag{3.5}
$$

It follows immediately that

$$
\begin{aligned}
\Theta_i^{A'}(t) = &\tau_A \alpha \Theta_i^A \sum_{k=1}^{n_A} \frac{k^2 p^A(k)}{\langle k \rangle_A} (1 - \varepsilon_k^A)(\theta_A)^k \Psi_A \\
&+ (1 - \alpha)\sigma_A \sum_{k=1}^{n_A} \frac{k p^A(k)}{\langle k \rangle_A} (1 - \varepsilon_k^A)(\theta_A)^k \Psi_A i^B - \gamma_A \Theta_i^A, \\
\Theta_i^{B'}(t) = &\tau_B \beta \Theta_i^B \sum_{l=1}^{n_B} \frac{l^2 p^B(l)}{\langle k \rangle_B} (1 - \varepsilon_l^B)(\theta_B)^l \Psi_B \\
&+ (1 - \beta)\sigma_B \sum_{l=1}^{n_B} \frac{l p^B(l)}{\langle k \rangle_B} (1 - \varepsilon_l^B)(\theta_B)^l \Psi_B i^A - \gamma_B \Theta_i^B.
\end{aligned}
\tag{3.6}
$$

From the above analysis, the rates of change of the fraction of infected individuals over time are obtained as

$$i^{A'}(t) = \tau_A \alpha \Theta_i^A \sum_{k=1}^{n_A} k p^A(k)(1 - \varepsilon_k^A)(\theta_A)^k \Psi_A$$

$$+ (1 - \alpha)\sigma_A \sum_{k=1}^{n_A} p^A(k)(1 - \varepsilon_k^A)(\theta_A)^k \Psi_A i^B - \gamma_A i^A,$$

$$i^{B'}(t) = \tau_B \beta \Theta_i^B \sum_{l=1}^{n_B} l p^B(l)(1 - \varepsilon_l^B)(\theta_B)^l \Psi_B$$

$$+ (1 - \beta)\sigma_B \sum_{l=1}^{n_B} p^B(l)(1 - \varepsilon_l^B)(\theta_B)^l \Psi_B i^A - \gamma_B i^B. \tag{3.7}$$

The above Eqs. (3.4), (3.6), and (3.7) constitute a low-dimensional model corresponding to model (2.2), and their initial values are $\theta_A(0) = 1$, $\Psi_A(0) = 1$, $\theta_B(0) = 1$, $\Psi_B(0) = 1$, $\Theta_i^A(0) = \sum_{k=1}^{n_A} \frac{k p^A(k)}{\langle k \rangle_A} \varepsilon_k^A$, $\Theta_i^B(0) = \sum_{l=1}^{n_B} \frac{l p^B(l)}{\langle k \rangle_B} \varepsilon_l^B$, $i^A(0) = \sum_{k=1}^{n_A} p^A(k)\varepsilon_k^A$, $i^B(0) = \sum_{l=1}^{n_B} p^B(l)\varepsilon_l^B$.

To calculate the basic reproduction number of the low-dimensional model, we use the next generation matrix method (Van den Driessche and Watmough 2002). At the disease-free equilibrium ($\theta_A = 1$, $\Psi_A = 1$, $\theta_B = 1$, $\Psi_B = 1$, $\Theta_i^A = 0$, $\Theta_i^B = 0$, $i^A = 0$, $i^B = 0$), one has

$$\begin{cases} \Theta_i^{A'}(t) = \tau_A \alpha \Theta_i^A \sum_{k=1}^{n_A} \frac{k^2 p^A(k)}{\langle k \rangle_A}(1 - \varepsilon_k^A) + (1 - \alpha)\sigma_A \sum_{k=1}^{n_A} \frac{k p^A(k)}{\langle k \rangle_A}(1 - \varepsilon_k^A)i^B - \gamma_A \Theta_i^A, \\ \Theta_i^{B'}(t) = \tau_B \beta \Theta_i^B \sum_{l=1}^{n_B} \frac{l^2 p^B(l)}{\langle k \rangle_B}(1 - \varepsilon_l^B) + (1 - \beta)\sigma_B \sum_{l=1}^{n_B} \frac{l p^B(l)}{\langle k \rangle_B}(1 - \varepsilon_l^B)i^A - \gamma_B \Theta_i^B, \\ i^{A'}(t) = \tau_A \alpha \Theta_i^A \sum_{k=1}^{n_A} k p^A(k)(1 - \varepsilon_k^A) + (1 - \alpha)\sigma_A \sum_{k=1}^{n_A} p^A(k)(1 - \varepsilon_k^A)i^B - \gamma_A i^A, \\ i^{B'}(t) = \tau_B \beta \Theta_i^B \sum_{l=1}^{n_B} l p^B(l)(1 - \varepsilon_l^B) + (1 - \beta)\sigma_B \sum_{l=1}^{n_B} p^B(l)(1 - \varepsilon_l^B)i^A - \gamma_B i^B. \end{cases}$$
$$\tag{3.8}$$

Let $\varepsilon_k^A \to 0$ ($k = 1, \ldots, n_A$), $\varepsilon_l^B \to 0$ ($l = 1, \ldots, n_B$), then we get the following matrix form

$$\begin{bmatrix} \Theta_i^{A'}(t) \\ \Theta_i^{B'}(t) \\ i^{A'}(t) \\ i^{B'}(t) \end{bmatrix} = (\mathcal{F}_1 - \mathcal{V}_1) \begin{bmatrix} \Theta_i^A(t) \\ \Theta_i^B(t) \\ i^A(t) \\ i^B(t) \end{bmatrix}, \tag{3.9}$$

where

$$\mathcal{F}_1 = \begin{bmatrix} \tau_A \alpha \frac{\langle k^2 \rangle_A}{\langle k \rangle_A} & 0 & 0 & (1 - \alpha)\sigma_A \\ 0 & \tau_B \beta \frac{\langle k^2 \rangle_B}{\langle k \rangle_B} & (1 - \beta)\sigma_B & 0 \\ \tau_A \alpha \langle k \rangle_A & 0 & 0 & (1 - \alpha)\sigma_A \\ 0 & \tau_B \beta \langle k \rangle_B & (1 - \beta)\sigma_B & 0 \end{bmatrix}, \quad \mathcal{V}_1 = \begin{bmatrix} \gamma_A & 0 & 0 & 0 \\ 0 & \gamma_B & 0 & 0 \\ 0 & 0 & \gamma_A & 0 \\ 0 & 0 & 0 & \gamma_B \end{bmatrix}.$$

The basic reproduction number $\mathcal{R}_0$ is the spectral radius of the matrix $\mathcal{F}_1 \mathcal{V}_1^{-1}$. Therefore, $\mathcal{R}_0$ is the maximum modulus of the roots of the following quaternion equation

$$\lambda^4 + a_3 \lambda^3 + a_2 \lambda^2 + a_1 \lambda + a_0 = 0, \tag{3.10}$$

where $a_3 = -\rho_{lA} - \rho_{lB}$, $a_2 = \rho_{lA}\rho_{lB} - \rho_{gA}\rho_{gB}$, $a_1 = \rho_{gA}\rho_{gB}\left(\rho_{lA} \frac{\langle k^2 \rangle_A - \langle k \rangle_A^2}{\langle k^2 \rangle_A} + \rho_{lB} \frac{\langle k^2 \rangle_B - \langle k \rangle_B^2}{\langle k^2 \rangle_B}\right)$, $a_0 = \rho_{lA}\rho_{lB}\rho_{gA}\rho_{gB}\left(\frac{(\langle k \rangle_A^2 - \langle k^2 \rangle_A)(\langle k^2 \rangle_B - \langle k \rangle_B^2)}{\langle k^2 \rangle_A \langle k^2 \rangle_B}\right)$. Here, $\rho_{gA} = \frac{(1-\beta)\sigma_B}{\gamma_A}$ and $\rho_{gB} = \frac{(1-\alpha)\sigma_A}{\gamma_B}$ represent the potential for transmission of disease from community A to community B and from community B to community A through casual contact, respectively. The definitions of ρ_{lA}, ρ_{lB} are the same as those in Eq. (3.1). In fact, we can obtain the roots of the quaternion equation (3.10) using the Ferrari's solution (see Appendix).

We discuss the basic reproduction number for some specific cases below.

1. $\alpha = 0$. In this case, the basic reproduction number $\mathcal{R}_0$ is the maximum modulus of the roots of the following cubic equation

$$\lambda^3 + b_2 \lambda^2 + b_1 \lambda + b_0 = 0,$$

where $b_2 = -\rho_{lB}$, $b_1 = -\frac{\sigma_A}{\gamma_B}\rho_{gA}$, $b_0 = \rho_{gA}\rho_{lB}\frac{\sigma_A(\langle k^2 \rangle_B - \langle k \rangle_B^2)}{\gamma_B \langle k^2 \rangle_B}$. Here, ρ_{lB} and ρ_{gA} are the same as those defined earlier. The solution of this cubic equation has been discussed in the literature (Wang et al. 2012). When $\beta = 0$, from the literature (Wang et al. 2012), we know that $\Delta > 0$, which gives $\mathcal{R}_0 = \sqrt{\frac{\sigma_B \sigma_A}{\gamma_A \gamma_B}}$. This is the same result as that obtained from the original model (2.2). When $\beta = 0$, the basic reproduction number with a similar approach to $\alpha = 0$ can be derived.

2. $\alpha = 1$, $0 < \beta \leq 1$. When $\alpha = 1$, it means that susceptible individuals in community A are restricted from moving. The basic reproduction number is $\mathcal{R}_0 = \max\{\rho_{lA}|_{\alpha=1}, \rho_{lB}\}$ by solving the quadratic equation $\lambda^2 - (\rho_{lA}|_{\alpha=1} + \rho_{lB})\lambda + \rho_{lA}|_{\alpha=1}\rho_{lB} = 0$, and this result is the same as the previous one. When $\beta = 1$, $0 < \alpha \leq 1$, similarly to the case of $\alpha = 1$, $0 < \beta \leq 1$, the value of the basic reproduction number appears again, that is, $\mathcal{R}_0 = \max\{\rho_{lA}, \rho_{lB}|_{\beta=1}\}$. In particular, when $\alpha = 1, \beta = 1$, the basic reproduction number is $\mathcal{R}_0 = \max\{\frac{\tau_A \langle k^2 \rangle_A}{\gamma_A \langle k \rangle_A}, \frac{\tau_B \langle k^2 \rangle_B}{\gamma_B \langle k \rangle_B}\}$.

3.3 Final epidemic size

The final size represents the proportion of individuals who ultimately become infected over the disease transmission process. The final size is an important indicator for analyzing the long-term dynamic behaviour of the disease. Moreover, obtaining the final size of the disease allows us to recognize the severity of the disease so that we can take more effective control measures to minimize the impact of the disease on human health and economic losses. Below, we calculate the final size equation of model (2.2). Additionally, we establish the existence and uniqueness of the solution to the final size equation, inspired by Magal et al. (2016) and Magal et al. (2018).

In model (2.2), let

$$\eta_k^A(t) = \sum_{j=1}^{n_A} \tau_A \alpha k \frac{j p^A(j)}{\langle k \rangle_A} i_j^A + \sum_{j=1}^{n_B}(1-\alpha)\sigma_A p^B(j) i_j^B, \tag{3.11}$$

and

$$\eta_l^B(t) = \sum_{j=1}^{n_B} \tau_B \beta l \frac{j p^B(j)}{\langle k \rangle_B} i_j^B + \sum_{j=1}^{n_A}(1-\beta)\sigma_B p^A(j) i_j^A. \tag{3.12}$$

The first and fourth equations in model (2.2) are then transformed as

$$\begin{cases} \dot{s}_k^A(t) = -s_k^A \eta_k^A, \\ \dot{s}_l^B(t) = -s_l^B \eta_l^B. \end{cases} \tag{3.13}$$

To facilitate the calculation of the final epidemic size, it is assumed that at the initial time $i_k^A(0) \ll s_k^A(0)$ and $i_l^B(0) \ll s_l^B(0)$. Integrating the above equation yields

$$\begin{cases} s_k^A(t) = s_k^A(0)exp(-\Phi_k^A), \\ s_l^B(t) = s_l^B(0)exp(-\Phi_l^B), \end{cases} \tag{3.14}$$

where

$$\Phi_k^A(t) = \int_0^t \eta_k^A(s)ds, \tag{3.15}$$

and

$$\Phi_l^B(t) = \int_0^t \eta_l^B(s)ds. \tag{3.16}$$

Integrating the third and sixth equations in model (2.2) from 0 to ∞ gives

$$\begin{cases} \dfrac{r_k^A(\infty)}{\gamma_A} = \displaystyle\int_0^\infty i_k^A(s)ds, \\ \dfrac{r_l^B(\infty)}{\gamma_B} = \displaystyle\int_0^\infty i_l^B(s)ds. \end{cases} \tag{3.17}$$

Integrating (3.11), (3.12) from 0 to ∞ and let $t \to \infty$ in (3.15) and (3.16) yields

$$\begin{cases} \Phi_k^A(\infty) = \displaystyle\sum_{j=1}^{n_A} \tau_A \alpha k \frac{j p^A(j)}{\langle k \rangle_A} \frac{r_j^A(\infty)}{\gamma_A} + \sum_{j=1}^{n_B}(1-\alpha)\sigma_A p^B(j)\frac{r_j^B(\infty)}{\gamma_B}, \\ \Phi_l^B(\infty) = \displaystyle\sum_{j=1}^{n_B} \tau_B \beta l \frac{j p^B(j)}{\langle k \rangle_B} \frac{r_j^B(\infty)}{\gamma_B} + \sum_{j=1}^{n_A}(1-\beta)\sigma_B p^A(j)\frac{r_j^A(\infty)}{\gamma_A}. \end{cases} \tag{3.18}$$

Since $s_k^A(\infty) = 1 - r_k^A(\infty) = s_k^A(0)exp(-\Phi_k^A(\infty))$ and $s_l^B(\infty) = 1 - r_l^B(\infty) = s_l^B(0)exp(-\Phi_l^B(\infty))$, one has

$$\begin{cases} z_k^A = 1 - s_k^A(0)exp(-\Phi_k^A(\infty)), \\ z_l^B = 1 - s_l^B(0)exp(-\Phi_l^B(\infty)). \end{cases} \tag{3.19}$$

Combining Eqs. (3.18) and (3.19), we have the following relations:

$$\begin{cases} \Phi_k^A(\infty) = \sum_{j=1}^{n_A} \tau_A \alpha k \dfrac{j p^A(j)}{\langle k \rangle_A \gamma_A} \left(1 - s_j^A(0)exp(-\Phi_j^A(\infty))\right) \\ \qquad\qquad + \sum_{j=1}^{n_B} \dfrac{(1-\alpha)\sigma_A p^B(j)}{\gamma_B} \left(1 - s_j^B(0)exp(-\Phi_j^B(\infty))\right), \\ \Phi_l^B(\infty) = \sum_{j=1}^{n_B} \tau_B \beta l \dfrac{j p^B(j)}{\langle k \rangle_B \gamma_B} \left(1 - s_j^B(0)exp(-\Phi_j^B(\infty))\right) \\ \qquad\qquad + \sum_{j=1}^{n_A} \dfrac{(1-\beta)\sigma_B p^A(j)}{\gamma_A} \left(1 - s_j^A(0)exp(-\Phi_j^A(\infty))\right). \end{cases} \tag{3.20}$$

In addition, rearranging the above equations gives

$$\Phi_k^A(\infty) = k\delta_A + \zeta_B, \ \Phi_l^B(\infty) = l\delta_B + \zeta_A,$$

where

$$\delta_A = \sum_{j=1}^{n_A} \tau_A \alpha \dfrac{j p^A(j)}{\langle k \rangle_A \gamma_A} \left(1 - s_j^A(0)exp(-j\delta_A - \zeta_B)\right),$$

$$\zeta_B = \sum_{j=1}^{n_B} \dfrac{(1-\alpha)\sigma_A p^B(j)}{\gamma_B} \left(1 - s_j^B(0)exp(-j\delta_B - \zeta_A)\right),$$

$$\delta_B = \sum_{j=1}^{n_B} \tau_B \beta \dfrac{j p^B(j)}{\langle k \rangle_B \gamma_B} \left(1 - s_j^B(0)exp(-j\delta_B - \zeta_A)\right),$$

$$\zeta_A = \sum_{j=1}^{n_A} \dfrac{(1-\beta)\sigma_B p^A(j)}{\gamma_A} \left(1 - s_j^A(0)exp(-j\delta_A - \zeta_B)\right).$$

The final size of the whole population of both communities A and B is

$$z = \nu \sum_{k=1}^{n_A} p^A(k) z_k^A + (1-\nu) \sum_{l=1}^{n_B} p^B(l) z_l^B$$

$$= v \sum_{k=1}^{n_A} p^A(k)\big(1 - s_k^A(0)exp(-k\delta_A - \zeta_B)\big)$$

$$+ (1-v)\sum_{l=1}^{n_B} p^B(l)\big(1 - s_l^B(0)exp(-l\delta_B - \zeta_A)\big)$$

$$= v\big\langle 1 - s_k^A(0)exp(-k\delta_A - \zeta_B)\big\rangle_A + (1-v)\big\langle 1 - s_l^B(0)exp(-l\delta_B - \zeta_A)\big\rangle_B, \tag{3.21}$$

where $v = \frac{N^A}{N^A+N^B}$, $1-v = \frac{N^B}{N^A+N^B}$, δ_A, ζ_B, δ_B and ζ_A can also be expressed as

$$\begin{cases} \rho_{lA} = \dfrac{\delta_A \langle k^2\rangle_A}{\Big\langle k\big(1 - s_k^A(0)exp(-k\delta_A - \zeta_B)\big)\Big\rangle_A}, \\[4mm] \rho_{gB} = \dfrac{\zeta_B}{\Big\langle 1 - s_l^B(0)exp(-l\delta_B - \zeta_A)\Big\rangle_B}, \\[4mm] \rho_{lB} = \dfrac{\delta_B \langle k^2\rangle_B}{\Big\langle l\big(1 - s_l^B(0)exp(-l\delta_B - \zeta_A)\big)\Big\rangle_B}, \\[4mm] \rho_{gA} = \dfrac{\zeta_A}{\Big\langle 1 - s_k^A(0)exp(-k\delta_A - \zeta_B)\Big\rangle_A}, \end{cases} \tag{3.22}$$

where $\langle g(k)\rangle_A = \sum_{k=1}^{n_A} g(k) p^A(k)$, $\langle g(l)\rangle_B = \sum_{l=1}^{n_B} g(l) p^B(l)$.

In the following, we prove that the solution of the final size equation (3.19) is unique.

Since $z_k^A = 1 - s_k^A(\infty)$, $z_l^B = 1 - s_l^B(\infty)$, Eq. (3.19) is equivalent to

$$\begin{cases} s_k^A(\infty) = s_k^A(0)exp\Big[\sum_{j=1}^{n_A} \dfrac{\tau_A \alpha k j p^A(j)}{\langle k\rangle_A \gamma_A}\big(s_j^A(\infty) - i_j^A(0) - s_j^A(0)\big) \\[4mm] \qquad\qquad + \sum_{j=1}^{n_B} \dfrac{(1-\alpha)\sigma_A p^B(j)}{\gamma_B}\big(s_j^B(\infty) - i_j^B(0) - s_j^B(0)\big)\Big], \\[4mm] s_l^B(\infty) = s_l^B(0)exp\Big[\sum_{j=1}^{n_B} \dfrac{\tau_B \beta l j p^B(j)}{\langle k\rangle_B \gamma_B}\big(s_j^B(\infty) - i_j^B(0) - s_j^B(0)\big) \\[4mm] \qquad\qquad + \sum_{j=1}^{n_A} \dfrac{(1-\beta)\sigma_B p^A(j)}{\gamma_A}\big(s_j^A(\infty) - i_j^A(0) - s_j^A(0)\big)\Big]. \end{cases} \tag{3.23}$$

We just need to prove the solution of Eq. (3.23) is unique. Write the vector form of Eq. (3.23) as

$$s(\infty) = exp\Big[diag\big(\mathcal{F}\mathcal{V}^{-1}(s(\infty) - s(0) - i(0))\big)\Big]s(0), \tag{3.24}$$

where $s(\infty) = \left[s_1^A(\infty), \ldots, s_{n_A}^A(\infty), s_1^B(\infty), \ldots, s_{n_B}^B(\infty)\right]^T$, $s(0) = \left[s_1^A(0), \ldots, s_{n_A}^A(0), s_1^B(0), \ldots, s_{n_B}^B(0)\right]^T$, $i(0) = \left[i_1^A(0), \ldots, i_{n_A}^A(0), i_1^B(0), \ldots, i_{n_B}^B(0)\right]^T$, $\mathcal{F}$ and $\mathcal{V}$ are the same as before.

We use the following notations in the next discussion. We define $X \leq Y$, if $X_k^A \leq Y_k^A$ and $X_l^B \leq Y_l^B$ for all $k = 1, \ldots, n_A, l = 1, \ldots, n_B$; $X < Y$, if $X \leq Y$ and $X_k^A < Y_k^A$ (or $X_l^B < Y_l^B$) for some $k = 1, \ldots, n_A$ (or $l = 1, \ldots, n_B$); $X \ll Y$, if $X_k^A < Y_k^A$ and $X_l^B < Y_l^B$ for all $k = 1, \ldots, n_A, l = 1, \ldots, n_B$. Defining a mapping $H : R^{n_A+n_B} \rightarrow R^{n_A+n_B}$:

$$H(X) = \left(H_1^A(X), \ldots, H_{n_A}^A(X), H_1^B(X), \ldots, H_{n_B}^B(X)\right)^T,$$

where $X = [X_1^A, \ldots, X_{n_A}^A, X_1^B, \ldots, X_{n_B}^B]^T \in R^{n_A+n_B}$,

$$\begin{cases} H_k^A(X) = s_k^A(0) \exp\left[\sum_{j=1}^{n_A} \frac{\tau_A \alpha k j p^A(j)}{\langle k \rangle_A \gamma_A}\left(X_j^A - i_j^A(0) - s_j^A(0)\right) \right. \\ \qquad\qquad \left. + \sum_{j=1}^{n_B} \frac{(1-\alpha)\sigma_A p^B(j)}{\gamma_B}\left(X_j^B - i_j^B(0) - s_j^B(0)\right)\right], k = 1, \ldots, n_A, \\ H_l^B(X) = s_l^B(0) \exp\left[\sum_{j=1}^{n_B} \frac{\tau_B \beta l j p^B(j)}{\langle k \rangle_B \gamma_B}\left(X_j^B - i_j^B(0) - s_j^B(0)\right) \right. \\ \qquad\qquad \left. + \sum_{j=1}^{n_A} \frac{(1-\beta)\sigma_B p^A(j)}{\gamma_A}\left(X_j^A - i_j^A(0) - s_j^A(0)\right)\right], l = 1, \ldots, n_B. \end{cases} \tag{3.25}$$

Based on the aforementioned definition, we further obtain

$$\begin{cases} \dfrac{\partial H_k^A(X)}{\partial X_j^A} = \dfrac{\tau_A \alpha k j p^A(j)}{\langle k \rangle_A \gamma_A} H_k^A(X), k = 1, \ldots, n_A, j = 1, \ldots, n_A, \\[2mm] \dfrac{\partial H_k^A(X)}{\partial X_j^B} = \dfrac{(1-\alpha)\sigma_A p^B(j)}{\gamma_B} H_k^A(X), k = 1, \ldots, n_A, j = 1, \ldots, n_B, \\[2mm] \dfrac{\partial H_l^B(X)}{\partial X_j^A} = \dfrac{(1-\beta)\sigma_B p^A(j)}{\gamma_A} H_l^B(X), l = 1, \ldots, n_B, j = 1, \ldots, n_A, \\[2mm] \dfrac{\partial H_l^B(X)}{\partial X_j^B} = \dfrac{\tau_B \beta l j p^B(j)}{\langle k \rangle_B \gamma_B} H_l^B(X), l = 1, \ldots, n_B, j = 1, \ldots, n_B, \end{cases}$$

and thus $D(H(X)) = diag(H(X))\mathcal{F}\mathcal{V}^{-1}$. From the above notation, it follows that when $X \leq Y$, then $X_k^A \leq Y_k^A$ and $X_l^B \leq Y_l^B$ for all $k = 1, \ldots, n_A, l = 1, \ldots, n_B$. By the definition of $H_k^A(X)$ and $H_l^B(X)$, it follows that $H_k^A(X) \leq H_k^A(Y)$ and $H_l^B(X) \leq H_l^B(Y)$. Same as above by the previous notation we get $H(X) \leq H(Y)$. This shows that $D(H(X))$ and $H(X)$ are monotonically increasing. Since $\frac{\tau_A \alpha k j p^A(j)}{\langle k \rangle_A \gamma_A} > 0$ and

$\frac{(1-\beta)\sigma_B p^A(j)}{\gamma_A} > 0$ for $0 < \alpha, \beta < 1, j, k = 1, \ldots, n_A$, $\frac{\tau_B \beta l j p^B(j)}{\langle k \rangle_B \gamma_B} > 0$ and $\frac{(1-\alpha)\sigma_A p^B(j)}{\gamma_B} > 0$ for $0 < \alpha, \beta < 1, j, l = 1, \ldots, n_B$, we know if $X \ll Y$, then $H(X) \ll H(Y)$. To sum up, for $0 \ll s(0), 0 \leq i(0)$, the following relation holds: $0 \ll H(0) \leq H(s(0)) \leq s(0)$.

By iteration, for any $\kappa \geq 1$ one has

$$0 \ll H(0) \leq \cdots \leq H^{\kappa+1}(0) \leq H^{\kappa+1}(s(0)) \leq \cdots \leq H(s(0)) \leq s(0).$$

Taking the limit to the above relation leads to

$$0 \ll \lim_{\kappa \to +\infty} H^{\kappa}(0) =: s^- \leq s^+ := \lim_{\kappa \to +\infty} H^{\kappa}(s(0)) \leq s(0).$$

According to H is continuous, we have $0 \ll H(s^-) = s^-$ and $H(s^+) = s^+ \leq s(0)$. From the above discussion, the following theorem is obtained.

Theorem 3.2 *If $0 < \alpha < 1, 0 < \beta < 1, \gamma_A > 0, \gamma_B > 0$, then $\mathcal{F}$ is a non-negative irreducible matrix. For model (2.2) with initial values $0 \ll s(0), 0 \leq i(0)$, the mapping H satisfies*

(1) $H(s(0)) = s(0)$ if and only if $i(0) = 0$;
(2) if $i(0) > 0$, then H has a unique fixed point $s(\infty)$ and $0 \ll s(\infty) < s(0)$.

Proof For (1), the necessity is obvious, and below we prove the sufficiency. When $H(s(0)) = s(0)$, it is implied from Eq. (3.24) that $\mathcal{F}\mathcal{V}^{-1}i(0) = 0$. Since $\mathcal{F}\mathcal{V}^{-1}$ is non-negative irreducible and $i(0) \geq 0$, one has $i(0) = 0$.

For (2), since $i(0) > 0$, we know $0 \ll H(s(0)) < s(0)$ and $s^+ < s(0)$. By the monotonicity of H, we further have $H(s^+) = s^+ \leq H(s(0))$. If $s^- = s^+$, then the result is obvious.

Now consider the case of $s^- < s^+$,

$$s^+ - s^- = H(s^+) - H(s^-) = \int_0^1 DH(s^- + m(s^+ - s^-))(s^+ - s^-)dm.$$

For any $0 \leq m \leq 1$, then

$$DH(s^- + m(s^+ - s^-))(s^+ - s^-) \leq DH(s^+)(s^+ - s^-).$$

Since $s^- < s^+$, one has

$$s^+ - s^- = \int_0^1 DH(s^- + m(s^+ - s^-))(s^+ - s^-)dm \leq DH(s^+)(s^+ - s^-).$$

It follows from the Perron-Frobenius theorem that there exists a left eigenvector $M \gg 0$ corresponding to the spectral radius $r(DH(s^+))$ of matrix $DH(s^+)$ such that

$$M^T(s^+ - s^-) \leq M^T DH(s^+)(s^+ - s^-) = r(DH(s^+))M^T(s^+ - s^-) \Rightarrow 1 \leq r(DH(s^+)).$$

Moreover,

$$H(s(0)) - s^+ = H(s(0)) - H(s^+) = \int_0^1 DH(s^+ + m(s(0) - s^+))(s(0) - s^+)dm$$
$$\geq DH(s^+)(s(0) - s^+).$$

So we get

$$M^T(H(s(0)) - s^+) \geq r(DH(s^+))M^T(s(0) - s^+).$$

Since $r(DH(s^+)) \geq 1$, it follows that

$$M^T H(s(0)) \geq M^T s(0).$$

We see that the above inequality contradicts $H(s(0)) < s(0)$. The theorem is proved. ∎

Therefore, we demonstrate that the solution of the final size equation (3.19) is unique.

In addition, we note that the method in Rass and Radcliffe (2003) can be also used to prove the existence and uniqueness of the solution to the final size equation. To see this, we rewrite Eq. (3.24) as

$$-\ln(1 - y_k) = \sum_{l=1}^{n_A+n_B} \gamma_{kl} y_l + a_k, \quad k = 1, 2, \ldots, n_A + n_B, \quad (3.26)$$

where

$$y_k = r_k^A(\infty) \text{ for } k = 1, 2, \ldots, n_A, \ y_k = r_{k-n_A}^B(\infty) \text{ for } k = n_A + 1, n_A + 2, \ldots, n_A + n_B,$$

$$\gamma_{kl} = \begin{cases} \dfrac{\tau_A \alpha k l p^A(l)}{\langle k \rangle_A \gamma_A}, & 1 \leq k \leq n_A, 1 \leq l \leq n_A, \\[2mm] \dfrac{(1 - \alpha)\sigma_A p^B(l - n_A)}{\gamma_B}, & 1 \leq k \leq n_A, n_A + 1 \leq l \leq n_A + n_B, \\[2mm] \dfrac{(1 - \beta)\sigma_B p^A(l)}{\gamma_A}, & n_A + 1 \leq k \leq n_A + n_B, 1 \leq l \leq n_A, \\[2mm] \dfrac{\tau_B \beta(k - n_A)(l - n_A)p^B(l - n_A)}{\langle k \rangle_B \gamma_B}, & n_A + 1 \leq k \leq n_A + n_B, n_A + 1 \leq l \leq n_A + n_B, \end{cases}$$

$$a_k = -\ln s_k^A(0) \geq 0 \text{ for } k = 1, 2, \ldots, n_A, \ a_k = -\ln s_{k-n_A}^B(0) \geq 0 \text{ for } k = n_A + 1, n_A + 2, \ldots,$$

$n_A + n_B$. Then, according to Theorem B.2 in Rass and Radcliffe (2003), the solution of the final size equation (3.19) is unique when $a_k > 0$. However, when $a_k = 0$, the final size equation has a zero solution. There is also a nonzero solution to the final size equation when both $a_k = 0$ and $\rho(\mathcal{F}\mathcal{V}^{-1}) > 1$ hold, but this is less biologically significant. □

Remark 3.3 It follows from the above that Eq. (3.24) can be rewritten as (3.26), and the matrix $\mathcal{F}\mathcal{V}^{-1}$ is non-negative irreducible and $\rho(\mathcal{F}\mathcal{V}^{-1})$ is finite, which satisfies

the condition of (1) in Theorem 3.2 in Rass and Radcliffe (2003). Then, $y_k = v_k$ is a solution of Eq. (3.26), where v_k represents the proportion of individuals with degree k who eventually suffer an epidemic. It follows that $y_k = v_k$ is a solution of Eq. (3.19). In our research, we adopted an approach of Magal et al. (2016) to establish the existence and uniqueness of the solution to the final size equation, as their method is considered more tivial and intuitive for practical applications compared to the approach presented in Rass and Radcliffe (2003).

From the expression of the final size we know that the final size is related to the degrees of the nodes in the network. We further investigate the relationship between them below. Inspired by the literature (Cui et al. 2022), we now use numerical simulations to analyze the case in which two communities have homogeneous degree distributions. In particular, community network A has delta degree distribution k_1 (all nodes have the same degrees), and community network B has delta degree distribution k_2. Rewrite (3.19) in the following form

$$F(z_{k_1}^A, z_{k_2}^B) = 1, \ G(z_{k_1}^A, z_{k_2}^B) = 1,$$

where

$$F(z_{k_1}^A, z_{k_2}^B) = \frac{1}{z_{k_1}^A}\left(1 - s_{k_1}^A(0)\exp\left(-\frac{\tau_A \alpha k_1}{\gamma_A}z_{k_1}^A - \frac{(1-\alpha)\sigma_A}{\gamma_B}z_{k_2}^B\right)\right),$$

$$G(z_{k_1}^A, z_{k_2}^B) = \frac{1}{z_{k_2}^B}\left(1 - s_{k_2}^B(0)\exp\left(-\frac{\tau_B \beta k_2}{\gamma_B}z_{k_2}^B - \frac{(1-\beta)\sigma_B}{\gamma_A}z_{k_1}^A\right)\right).$$

$$(3.27)$$

Moreover, it is easily confirmed that the basic reproduction number in this case is $\mathcal{R}_0 = \frac{1}{2}\left(\frac{\tau_A \alpha k_1}{\gamma_A} + \frac{\tau_B \beta k_2}{\gamma_B}\right) + \frac{1}{2}\sqrt{\left(\frac{\tau_A \alpha k_1}{\gamma_A} - \frac{\tau_B \beta k_2}{\gamma_B}\right)^2 + \frac{4(1-\alpha)(1-\beta)\sigma_A\sigma_B}{\gamma_A \gamma_B}}$. To obtain the relationship between $\mathcal{R}_0$ and α, β, calculating $\frac{\partial \mathcal{R}_0}{\partial \alpha} > 0$ gives $\tau_A k_1 \sqrt{C} + \frac{\tau_A k_1}{\gamma_A \gamma_B}(\tau_A \alpha k_1 \gamma_B - \tau_B \beta k_2 \gamma_A) - \frac{2(1-\beta)\sigma_A\sigma_B}{\gamma_B} > 0$, where $C = \left(\frac{\tau_A \alpha k_1}{\gamma_A} - \frac{\tau_B \beta k_2}{\gamma_B}\right)^2 + \frac{4(1-\alpha)(1-\beta)\sigma_A\sigma_B}{\gamma_A \gamma_B}$, then $\mathcal{R}_0$ increases as α increases. Otherwise, it decreases as α increases. Calculating $\frac{\partial \mathcal{R}_0}{\partial \beta} > 0$ yields $\tau_B k_2 \sqrt{C} + \frac{\tau_B k_2}{\gamma_A \gamma_B}(\tau_A \alpha k_1 \gamma_B - \tau_B \beta k_2 \gamma_A) - \frac{2(1-\alpha)\sigma_A\sigma_B}{\gamma_A} > 0$, then $\mathcal{R}_0$ increases as β increases.

In fact, the relationship between $\mathcal{R}_0$ and α, β is complex (non-monotonous), as revealed by the above analysis. To explore this relationship, we calculated the basic reproduction number $\mathcal{R}_0$ with different values of α (the contribution of disease transmission through intra-community A) and β (the contribution of disease transmission through intra-community B). Specifically, we used the parameter values $k_1 = 8, k_2 = 12, \tau_A = 0.3, \tau_B = 0.2, \sigma_A = 0.4, \sigma_B = 0.3, \gamma_A = 0.4, \gamma_B = 0.4$, and the initial values $s_{k_1}^A(0) = 0.998, s_{k_2}^B(0) = 0.995, i_{k_1}^A(0) = 0.002, i_{k_2}^B(0) = 0.005$. Results are shown in Fig. 2. It illustrates that the relationship between $\mathcal{R}_0$ and β (or α) is non-monotonous ($\mathcal{R}_0$ can either increase or decrease with β (or α)), when α (or β) is fixed. For example, when $\beta \in [0.9, 1]$, $\mathcal{R}_0$ decreases as α increases, while $\mathcal{R}_0$ is also a decreasing function of β when $\alpha \in [0.92, 1]$. The results suggest that,
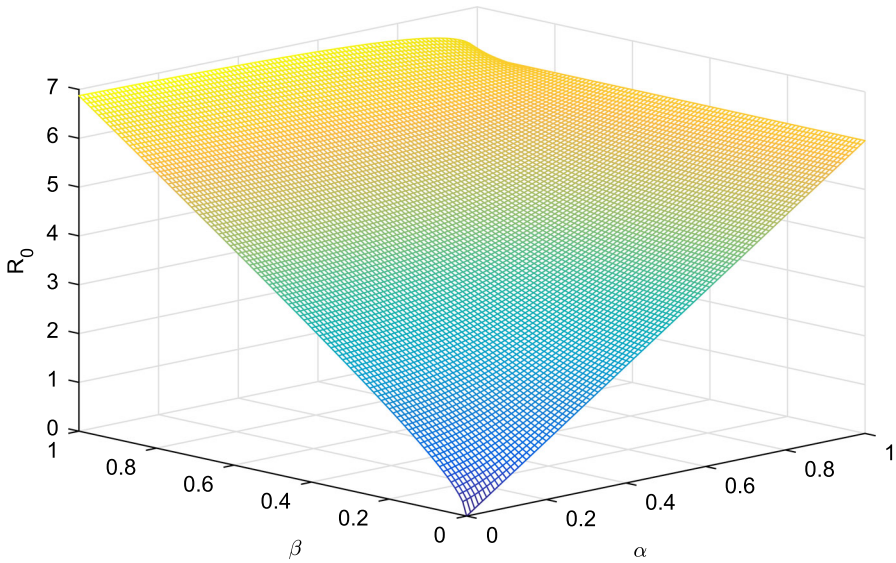
Fig. 2 Changes in the basic reproduction number $\mathcal{R}_0$ with α (the contribution of disease transmission through intra-community A) and β (the contribution of disease transmission through intra-community B)

in scenarios with restricted movement of susceptible individuals within a community, $\mathcal{R}_0$ does not follow a simple monotonous relationship, indicating that an unbending decrease in the movement of susceptible individuals may increase the $\mathcal{R}_0$.

In order to better analyze the relationship between the basic reproduction number and the parameters α and β, we give the following expanded model:

$$
\begin{cases}
\dot{s}_k^A(t) = -\tau_A \alpha k s_k^A \Theta_i^A - \tilde{\alpha} \sigma_A s_k^A i^B, \\
\dot{i}_k^A(t) = \tau_A \alpha k s_k^A \Theta_i^A + \tilde{\alpha} \sigma_A s_k^A i^B - \gamma_A i_k^A, \\
\dot{r}_k^A(t) = \gamma_A i_k^A, \\
\dot{s}_l^B(t) = -\tau_B \beta l s_l^B \Theta_i^B - \tilde{\beta} \sigma_B s_l^B i^A, \\
\dot{i}_l^B(t) = \tau_B \beta l s_l^B \Theta_i^B + \tilde{\beta} \sigma_B s_l^B i^A - \gamma_B i_l^B, \\
\dot{r}_l^B(t) = \gamma_B i_l^B,
\end{cases}
\tag{3.28}
$$

where α (β) and $\tilde{\alpha}$ ($\tilde{\beta}$) represent the flow of population within community A (B) and the flow of population from community A (B) to community B (A), respectively. The other parameters are the same as in the model (2.2).

When community network A has delta degree distribution k_1 and community network B has delta degree distribution k_2, the basic reproduction number for model (3.28) is $\tilde{R}_0 = \frac{1}{2}\left(\frac{\tau_A \alpha k_1}{\gamma_A} + \frac{\tau_B \beta k_2}{\gamma_B}\right) + \frac{1}{2}\sqrt{\left(\frac{\tau_A \alpha k_1}{\gamma_A} - \frac{\tau_B \beta k_2}{\gamma_B}\right)^2 + \frac{4\tilde{\alpha}\tilde{\beta}\sigma_A \sigma_B}{\gamma_A \gamma_B}}$. By calculation, one has $\frac{\partial \tilde{R}_0}{\partial \alpha} = \frac{\tau_A k_1}{2\gamma_A}\left(1 + \left(\frac{\tau_A \alpha k_1}{\gamma_A} - \frac{\tau_B \beta k_2}{\gamma_B}\right)\frac{1}{\sqrt{D}}\right), \frac{\partial \tilde{R}_0}{\partial \beta} = \frac{\tau_B k_2}{2\gamma_B}\left(1 - \left(\frac{\tau_A \alpha k_1}{\gamma_A} - \frac{\tau_B \beta k_2}{\gamma_B}\right)\frac{1}{\sqrt{D}}\right),$

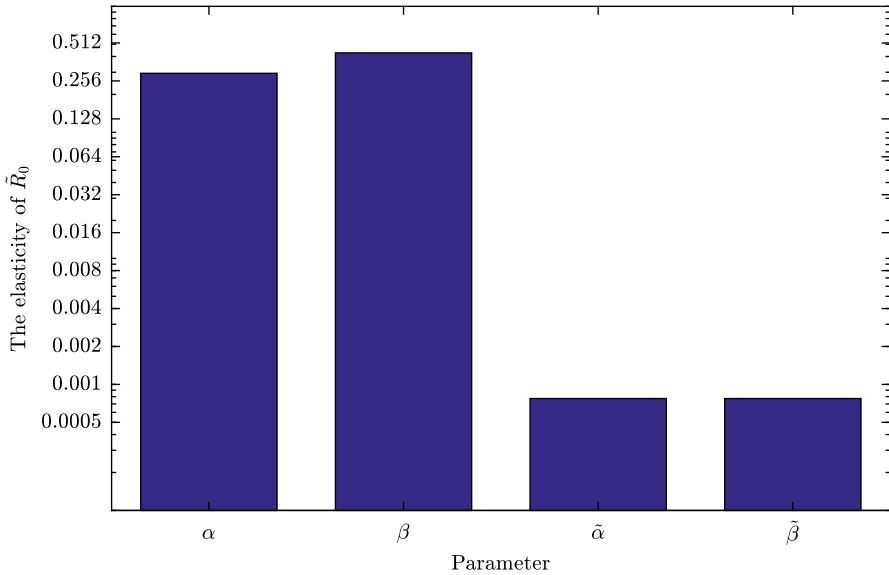**Fig. 3** Effect of several relevant parameters on $\tilde{R}_0$

$\frac{\partial \tilde{R}_0}{\partial \tilde{\alpha}} = \frac{\tilde{\beta}\sigma_A\sigma_B}{\gamma_A\gamma_B}\frac{1}{\sqrt{D}} > 0$ and $\frac{\partial \tilde{R}_0}{\partial \tilde{\beta}} = \frac{\tilde{\alpha}\sigma_A\sigma_B}{\gamma_A\gamma_B}\frac{1}{\sqrt{D}} > 0$, where $D = \left(\frac{\tau_A\alpha k_1}{\gamma_A} - \frac{\tau_B\beta k_2}{\gamma_B}\right)^2 +$ $\frac{4\tilde{\alpha}\tilde{\beta}\sigma_A\sigma_B}{\gamma_A\gamma_B}$. From this, we conclude that $\tilde{R}_0$ is monotonically increasing with $\tilde{\alpha}$ and $\tilde{\beta}$ while it is non-monotonically related to α and β. In order to reveal which of the parameters, namely α, $\tilde{\alpha}$, β, and $\tilde{\beta}$, is more sensitive to basic reproduction number $\tilde{R}_0$, we performed a sensitivity analysis of $\tilde{R}_0$ to α, $\tilde{\alpha}$, β, and $\tilde{\beta}$. Results are shown in Fig. 3. Here, we use the same values for the other parameters as in Fig. 2. As can be seen from Fig. 3, $\tilde{R}_0$ is more sensitive to α and β, and β has a greater impact on $\tilde{R}_0$ than α. This phenomenon could be attributed to the slightly larger degree distribution in community B compared to that in community A. Additionally, $\tilde{\alpha}$ and $\tilde{\beta}$ have almost the same impact on $\tilde{R}_0$. Therefore, from the perspective of controlling the outbreak of an epidemic, our most basic task is to control contacts among individuals within communities, but we must also not overlook contacts between individuals across different communities.

Figure 4 reveals the final sizes are determined by the intersection of $F = 1$ and $G = 1$ for three sets of degrees (k_1, k_2). Given the parameters: $\tau_A = 0.3$, $\tau_B = 0.2$, $\sigma_A = 0.4$, $\sigma_B = 0.3$, $\beta = 0.4$, $\alpha = 0.3$, $\gamma_A = 0.4$, $\gamma_B = 0.4$, $N^A = 5000$, $N^B = 5000$, and the initial values $s_{k_1}^A(0) = 0.998$, $s_{k_2}^B(0) = 0.995$, $i_{k_1}^A(0) = 0.002$, $i_{k_2}^B(0) = 0.005$, the left column of Fig. 4 shows the values of $z_{k_1}^A$, $z_{k_2}^B$ are determined by Eq. (3.27), as the intersection of $F = 1$ and $G = 1$ (marked with red dots); the right column shows the epidemic curves of recovered individuals, which are simulation results of system (2.2).

For the classical SIR model, the final size z is related to the basic reproduction number $\mathcal{R}_0$ as follows: $z = 1 - (1 - \varepsilon)e^{-\mathcal{R}_0 z}$, where $0 \leq \varepsilon \ll 1$ is the initial relative density of infected individuals. Let $f(z) = 1 - (1 - \varepsilon)e^{-\mathcal{R}_0 z}$, where $z \in [0, 1]$ and
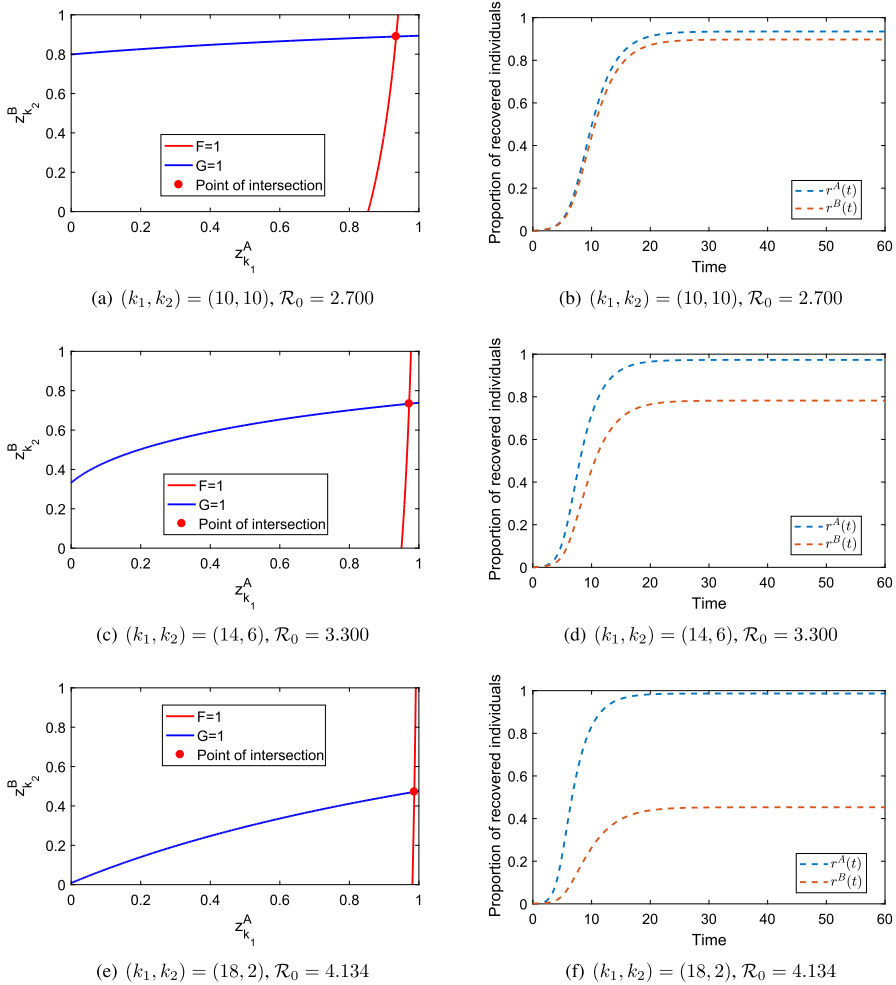
(a) $(k_1, k_2) = (10, 10)$, $\mathcal{R}_0 = 2.700$

(b) $(k_1, k_2) = (10, 10)$, $\mathcal{R}_0 = 2.700$

(c) $(k_1, k_2) = (14, 6)$, $\mathcal{R}_0 = 3.300$

(d) $(k_1, k_2) = (14, 6)$, $\mathcal{R}_0 = 3.300$

(e) $(k_1, k_2) = (18, 2)$, $\mathcal{R}_0 = 4.134$

(f) $(k_1, k_2) = (18, 2)$, $\mathcal{R}_0 = 4.134$

Fig. 4 The left column shows the final sizes at the three sets of degrees (k_1, k_2) represented by the intersection of $F = 1$ and $G = 1$. The right column shows the proportion of recovered individuals in communities A, B under the three sets of degrees (k_1, k_2)

$f(z)$ is continuous. Then we have the value of $f(z)$ for both end points of variable z: $f(0) = \varepsilon \geq 0$ and $f(1) = 1 - (1 - \varepsilon)e^{-\mathcal{R}_0} < 1$. This implies that the graph of $f(z)$ starts on or above the diagonal, and ends below the diagonal, resulting in intersections with the diagonal. Since $f'(z) = \mathcal{R}_0(1-\varepsilon)e^{-\mathcal{R}_0 z} > 0$, $f''(z) = -\mathcal{R}_0^2(1-\varepsilon)e^{-\mathcal{R}_0 z} < 0$, $f(z)$ is a concave function. When $\varepsilon = 0$, $f(z)$ intersects the diagonal at two points, namely the origin and $z^* \in [0, 1]$; when $\varepsilon > 0$, $f(z)$ intersects the diagonal only at z^*, a single positive solution in the interval $[0, 1]$. Therefore, the final size equation has either one trivial and one positive solution in the interval $[0, 1]$, or only one positive solution.
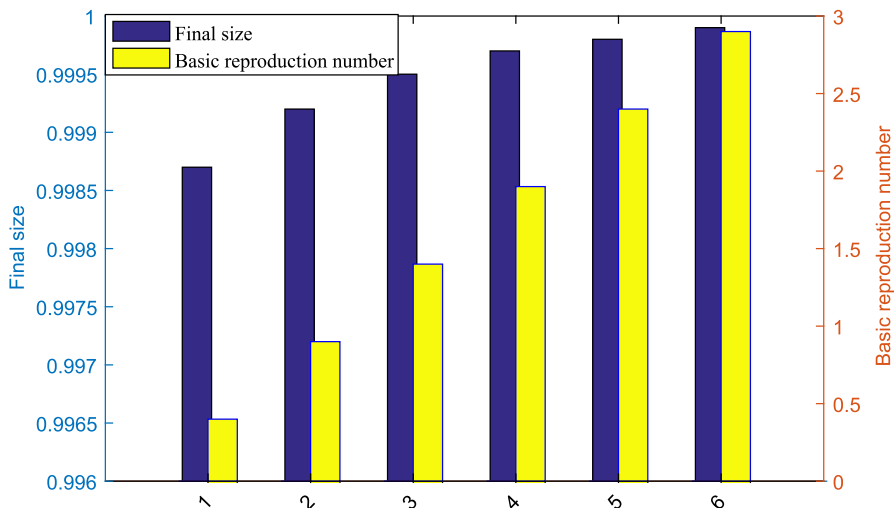
Fig. 5 Graph of the final size z with respect to the basic reproduction number $\mathcal{R}_0$ for the classical SIR model, which shows that z and $\mathcal{R}_0$ are positively correlated. Here, the relative density of the initially infected individuals is $\varepsilon = 0.002$

When studying epidemic models, the final size z and the basic reproduction number $\mathcal{R}_0$ are of great interest. It is common believed that reducing the value of $\mathcal{R}_0$ can decrease the final size z of the infected population, which is consistent with the positive relationship revealed in Fig. 5. Efforts to prevent and control epidemics have traditionally focused on reducing the basic reproduction number $\mathcal{R}_0$. However, as shown in Fig. 5, if the basic reproduction number is greater than 1, then the outbreak is inevitable. Therefore, it is more practical and effective to implement public health interventions to reduce the infected population rather than focusing solely on reducing $\mathcal{R}_0$. This can be achieved by regulating interactions among individuals.

The classical SIR model predicts a positive correlation between the final size z and the basic reproduction number $\mathcal{R}_0$. However, in our two-community model with homogeneous degree distributions, this relationship may be reversed and become negatively correlated when varying the degrees (k_1, k_2), as depicted in Fig. 6. In this way taking relevant measures to reduce the value of $\mathcal{R}_0$ will in turn lead to higher infected population. Furthermore, all the values of the basic reproduction number shown in Fig. 6 are greater than 1, indicating that the outbreak of infectious disease is unavoidable. Given such premise, the best strategy is to focus on reducing the number of infected individuals, thereby mitigating the impact of the outbreak.

In addition to the above method of calculating the final size, we can also calculate the final size of the disease through the reduced-dimensional model. The specific calculation process is as follows.
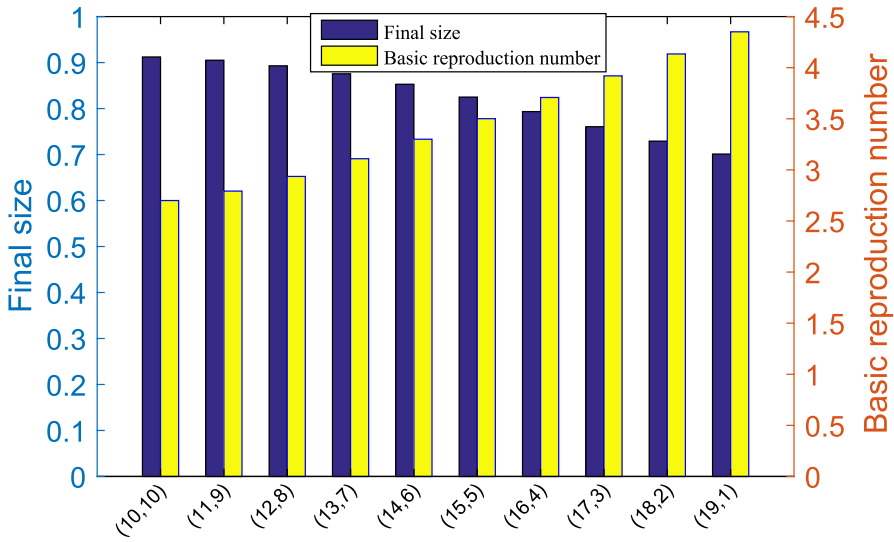
From Eq. (3.4), we have

Fig. 6 Graph of the evolution of the total final size z and the basic reproduction number $\mathcal{R}_0$ with different sets of degrees (k_1, k_2)

$$\ln \theta_A(t) = -\tau_A \alpha \int_0^t \Theta_i^A(s) ds, \quad \ln \Psi_A(t) = -(1-\alpha)\sigma_A \int_0^t i^B(s) ds,$$

$$\ln \theta_B(t) = -\tau_B \beta \int_0^t \Theta_i^B(s) ds, \quad \ln \Psi_B(t) = -(1-\beta)\sigma_B \int_0^t i^A(s) ds.$$

$$(3.29)$$

Since $\Theta_i^{A'}(t) + \Theta_s^{A'}(t) = -\gamma_A \Theta_i^A(t)$ and $\Theta_i^{B'}(t) + \Theta_s^{B'}(t) = -\gamma_B \Theta_i^B(t)$, integrating them yields

$$\int_0^t \Theta_i^A(s) ds = \frac{1}{\gamma_A}\left(1 - (\Theta_i^A + \Theta_s^A)\right), \quad \int_0^t \Theta_i^B(s) ds = \frac{1}{\gamma_B}\left(1 - (\Theta_i^B + \Theta_s^B)\right).$$

$$(3.30)$$

After inserting Eq. (3.30) into Eq. (3.29), one has

$$\ln \theta_A(t) = \frac{\tau_A \alpha}{\gamma_A}\left(\Theta_i^A + \Theta_s^A - 1\right), \quad \ln \theta_B(t) = \frac{\tau_B \beta}{\gamma_B}\left(\Theta_i^B + \Theta_s^B - 1\right). \quad (3.31)$$

From the definitions of Θ_s^A and Θ_s^B, it follows that

$$\Theta_s^A(\infty) = \sum_{k=1}^{n_A} \frac{k p^A(k)}{\langle k \rangle_A}(1 - \varepsilon_k^A)(\theta_A(\infty))^k \Psi_A(\infty),$$

$$\Theta_s^B(\infty) = \sum_{l=1}^{n_B} \frac{l p^B(l)}{\langle k \rangle_B} (1 - \varepsilon_l^B)(\theta_B(\infty))^l \Psi_B(\infty). \tag{3.32}$$

Since $\dot{r}_k^A(t) = \gamma_A i_k^A(t)$, $\dot{r}_l^B(t) = \gamma_B i_l^B(t)$, then

$$r_k^A(\infty) = \gamma_A \int_0^\infty i_k^A(s)ds, \ \ r_l^B(\infty) = \gamma_B \int_0^\infty i_l^B(s)ds.$$

Recall that the final size of community A and community B satisfies

$$z^A = r^A(\infty) - r^A(0) = \sum_{k=1}^{n_A} p^A(k) r_k^A(\infty) = \gamma_A \int_0^\infty i^A(s)ds,$$
$$z^B = r^B(\infty) - r^B(0) = \sum_{l=1}^{n_B} p^B(l) r_l^B(\infty) = \gamma_B \int_0^\infty i^B(s)ds. \tag{3.33}$$

From Eqs. (3.29) and (3.33), one has

$$\Psi_A(\infty) = exp\left(-\frac{(1-\alpha)\sigma_A}{\gamma_B} z^B\right), \ \ \Psi_B(\infty) = exp\left(-\frac{(1-\beta)\sigma_B}{\gamma_A} z^A\right). \tag{3.34}$$

And, from Eqs. (3.31) and (3.32), we know

$$\theta_A(\infty) = exp\left[\frac{\tau_A \alpha}{\gamma_A}\left(\sum_{k=1}^{n_A} \frac{k p^A(k)}{\langle k \rangle_A}(1 - \varepsilon_k^A)(\theta_A(\infty))^k \Psi_A(\infty) - 1\right)\right],$$
$$\theta_B(\infty) = exp\left[\frac{\tau_B \beta}{\gamma_B}\left(\sum_{l=1}^{n_B} \frac{l p^B(l)}{\langle k \rangle_B}(1 - \varepsilon_l^B)(\theta_B(\infty))^l \Psi_B(\infty) - 1\right)\right]. \tag{3.35}$$

In addition, the final size of the disease can be expressed as

$$z^A = 1 - s^A(\infty) = 1 - \sum_{k=1}^{n_A}(1 - \varepsilon_k^A) p^A(k)(\theta_A(\infty))^k \Psi_A(\infty),$$
$$z^B = 1 - s^B(\infty) = 1 - \sum_{l=1}^{n_B}(1 - \varepsilon_l^B) p^B(l)(\theta_B(\infty))^l \Psi_B(\infty). \tag{3.36}$$

The overall final epidemic size of the two communities is

$$
\begin{aligned}
z &= \nu z^A + (1-\nu) z^B \\
&= 1 - \Big(\nu \sum_{k=1}^{n_A} (1 - \varepsilon_k^A) p^A(k) (\theta_A(\infty))^k \Psi_A(\infty) \\
&\quad + (1-\nu) \sum_{l=1}^{n_B} (1 - \varepsilon_l^B) p^B(l) (\theta_B(\infty))^l \Psi_B(\infty) \Big),
\end{aligned} \tag{3.37}
$$

where $\nu = \frac{N^A}{N^A + N^B}$ and $1 - \nu = \frac{N^B}{N^A + N^B}$.

From the above, we see that Eq. (3.35) has a low dimension, making it suitable for numerical computations in large-scale networks. It can be solved by iteration. Furthermore, if $\varepsilon_k^A \approx 0$, $\varepsilon_l^B \approx 0$, then $\theta_A(\infty) \approx 1$, $\theta_B(\infty) \approx 1$, $\Psi_A(\infty) \approx 1$, $\Psi_B(\infty) \approx 1$, $z^A \approx 0$ and $z^B \approx 0$ is the solution of Eqs. (3.34)–(3.36) in the disease-free state.

4 Numerical simulations

In Sect. 3 we analyzed the basic reproduction number $\mathcal{R}_0$ and the final size z. In this section, we further specify factors affecting $\mathcal{R}_0$ and z, and figure out how their values will change when the network obeys the Power-law distribution $p^q(k) = Ck^{-3}$ (C satisfies $\sum_{k=1}^{n_q} p^q(k) = 1$, $q \in \{A, B\}$) and Poisson distribution $p^q(k) = \frac{(1.4)^k e^{-1.4}}{k!}$ for $k = 1, \ldots, n_q (q \in \{A, B\})$ through simulations. We choose the parameters $\gamma_A = 0.4$, $\gamma_B = 0.4$, $\alpha = 0.4$ or in $(0, 1)$, $\beta = 0.4$ or in $(0, 1)$, $\tau_A = 0.2$ or in $(0, 1)$, $\tau_B = 0.2$ or in $(0, 1)$, $\sigma_A = 0.3$ or in $(0, 1)$ and $\sigma_B = 0.3$ or in $(0, 1)$. Let the maximum degree of community A be $n_A = 100$ and the maximum degree of community B be $n_B = 200$. By fixing two parameters among $\tau_A, \tau_B, \sigma_A, \sigma_B$ and varying the other two parameters, we generate four contour plots of the network obeying Power-law distribution and Poisson distribution, respectively. Figures 7 and 8 illustrate that τ_A (τ_B) always has a greater impact on $\mathcal{R}_0$ than that of σ_A (σ_B), regardless of whether the contact networks of both communities obey the Power-law distribution or Poisson distribution. This result can be explained by the fact that contacts among people within the community are more frequent than contacts between communities during the epidemic. Hence, people needs to prioritize the attention towards the contacts among individuals within a community during the outbreak of epidemics, as this can effectively reduce the likelihood and severity of disease transmission. Figure 9 indicates that the impact of τ_B on $\mathcal{R}_0$ is slightly greater than that of τ_A on $\mathcal{R}_0$ as n_B is larger than n_A (There are more contacts among people in community B than among people in community A). This is consistent with reality: an epidemic spreads faster in a more crowded place. Figure 10 shows that σ_A and σ_B have almost equal influence on $\mathcal{R}_0$, which means that two transmission pathways of the disease between communities have the same effect on the epidemic. Furthermore, we observe that the value of $\mathcal{R}_0$ is marginally higher when the contact networks of both communities obey a Power-law distribution than when they obey a Poisson distribution with the same parameter values. This implies
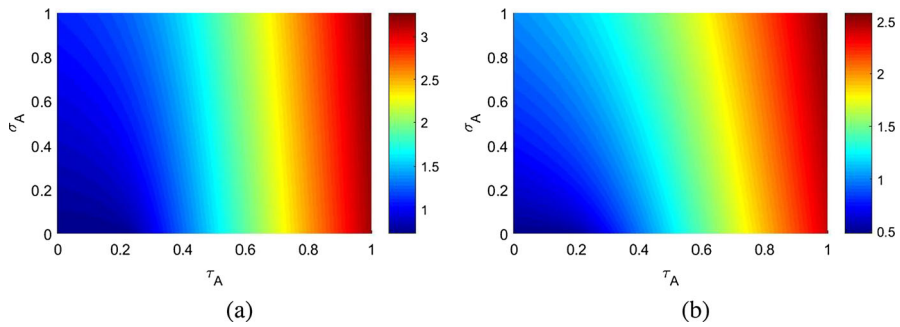
Fig. 7 Contour plots of $\mathcal{R}_0$ for parameters τ_A (disease transmission probability within community A) and σ_A (disease transmission probability from community B to community A): **a** the contact networks of both communities obey a Power-law distribution; **b** the contact networks of both communities obey a Poisson distribution
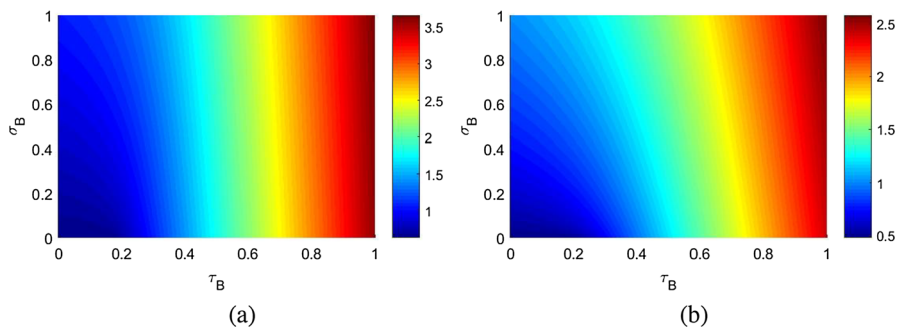

Fig. 8 Contour plots of $\mathcal{R}_0$ for parameters τ_B (disease transmission probability within community B) and σ_B (disease transmission probability from community A to community B): **a** the contact networks of both communities obey a Power-law distribution; **b** the contact networks of both communities obey a Poisson distribution

the larger heterogeneity of the degree distribution may lead to higher risk of disease outbreaks.

To show the relative significance of certain model parameters on the basic reproduction number $\mathcal{R}_0$, a sensitivity analysis is conducted on our model, and the results are presented in Fig. 11. As evident from Fig. 11, the probabilities of transmission of disease, namely, τ_A, τ_B, σ_A, and σ_B, are relatively more sensitive parameters with respect to $\mathcal{R}_0$. The recovery rates γ_A and γ_B have almost the same negative effects on $\mathcal{R}_0$. Moreover, the impact of intra-community disease transmission on $\mathcal{R}_0$ is slightly greater than that of inter-community transmission, and both transmissions have a significant effect. Figure 11 also shows that the transmission rates within a community, represented by τ_A and τ_B, have a relatively stronger impact on $\mathcal{R}_0$ than the rates between communities, represented by σ_A and σ_B. Interestingly, we found that the transmission rates from community A to B and from community B to A, i.e., σ_A and σ_B, have almost equal impact on $\mathcal{R}_0$. All these sensitivity analysis suggests that the fundamental approach to controlling the spread of epidemics is to control the contacts of individuals within a community. However, relying solely on controlling individuals'
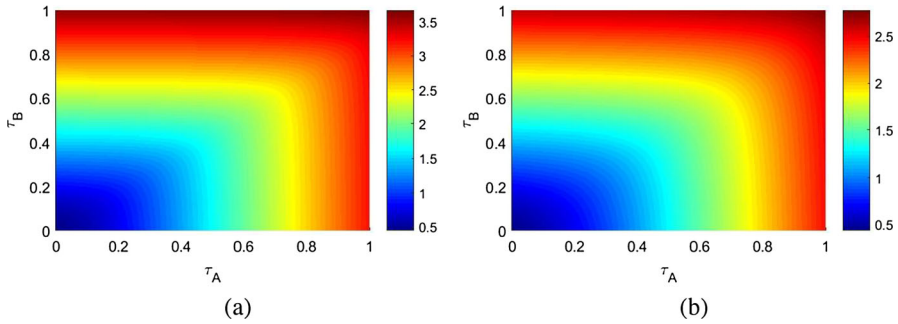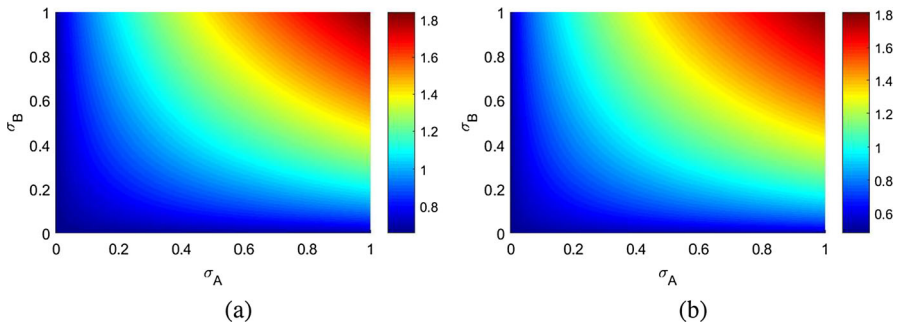
Fig. 9 Contour plots of $\mathcal{R}_0$ for parameters τ_A (disease transmission probability within community A) and τ_B (disease transmission probability within community B): **a** the contact networks of both communities obey a Power-law distribution; **b** the contact networks of both communities obey a Poisson distribution

Fig. 10 Contour plots of $\mathcal{R}_0$ for parameters σ_A (disease transmission probability from community B to community A) and σ_B (disease transmission probability from community A to community B): **a** the contact networks of both communities obey a Power-law distribution; **b** the contact networks of both communities obey a Poisson distribution

contacts within communities may not be the most effective strategy, and other factors should be considered.

The threshold value of $\mathcal{R}_0 = 1$ given two network distributions, under different value combinations of disease transmission contribution parameters α and β, is illustrated in Fig. 12. For the contact networks of both communities follow a Power-law distribution, the blue curve represents $\mathcal{R}_0 = 1$, with the region to the bottom left indicating $\mathcal{R}_0$ values smaller than 1, and the region to the top right indicating $\mathcal{R}_0$ values greater than 1. On the other hand, if the contact networks of both communities follow a Poisson distribution, there will be a higher chance that $\mathcal{R}_0 < 1$ as the corresponding region is larger.

Figures 13 and 14 present the variation of the final epidemic size under two degree distributions, presented here as the changes in the number of individuals affected by disease, given different values of transmission probabilities τ_A, τ_B, σ_A and σ_B. Here, in addition to the parameters given in the numerical simulation section, we choose $\theta_A(0) = 0.8$, $\theta_B(0) = 0.8$, $z^A(0) = 0.1$, $z^B(0) = 0.1$, $\varepsilon_k^A = 0.002$, $k = 1, \ldots, 100$, $\varepsilon_l^B = 0.005$, $l = 1, \ldots, 200$. We assume that community A and com-
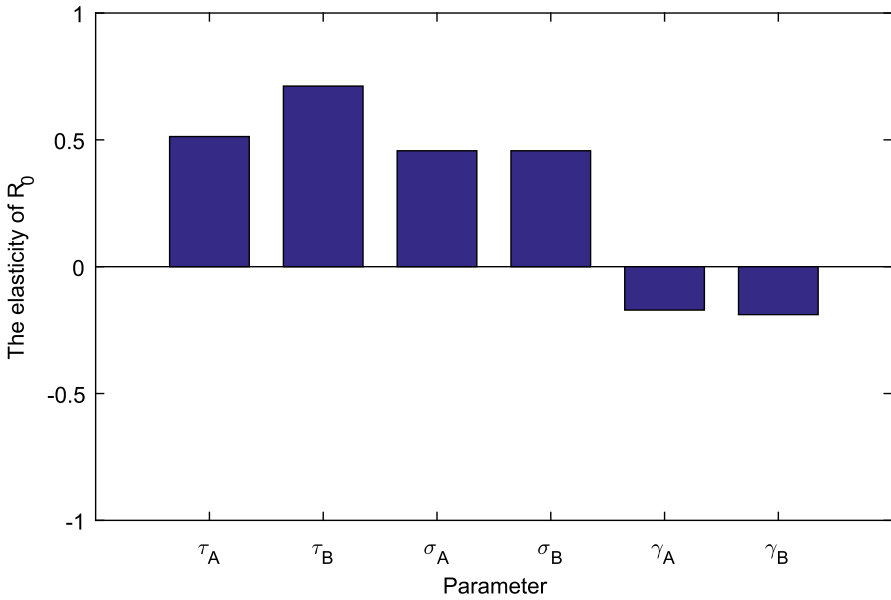
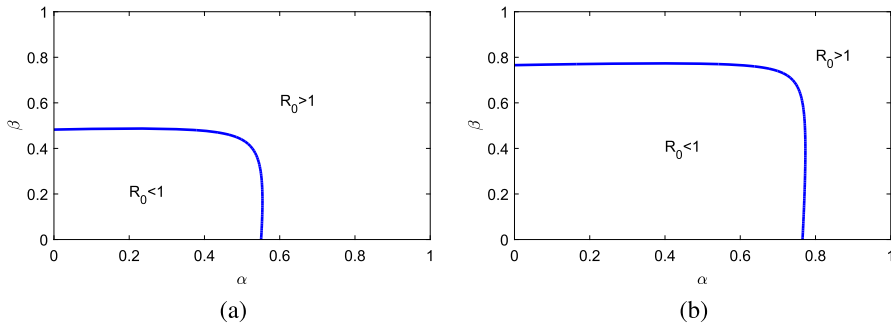**Fig. 11** Effect of several relevant parameters on $\mathcal{R}_0$

Fig. 12 Changes in the value of $\mathcal{R}_0$ with α (the contribution of disease transmission through intra-community A) and β (the contribution of disease transmission through intra-community B): **a** the contact networks of both communities obey a Power-law distribution; **b** the contact networks of both communities obey a Poisson distribution

munity B have 5000 individuals for each. Although the two models have the same parameters and mean degrees, these figures suggest that the model in which the contact networks of both communities obey a Power-law distribution has a smaller final size than the one in which the contact networks of both communities obey a Poisson distribution. This means that the heterogeneity of the degree distribution reduces the final size. Figure 15 reveals the effect of α and β on the final size under two degree distributions. We find that the model in which the contact networks of both communities obey the Poisson distribution has a greater final size than the one in which the contact
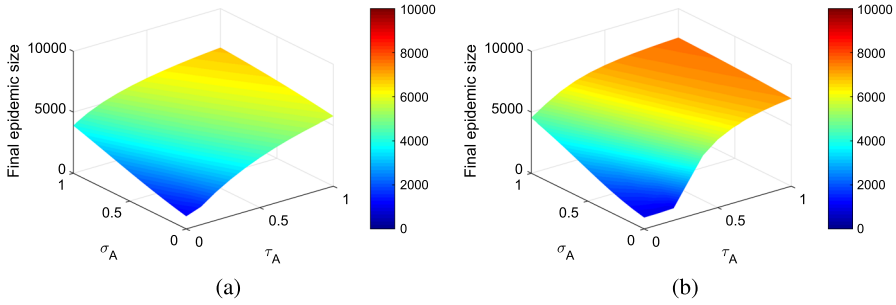
Fig. 13 The relation of the final size (i.e. the number of individuals affected by disease) to τ_A (disease transmission probability within community A) and σ_A (disease transmission probability from community B to community A): **a** the contact networks of both communities obey a Power-law distribution; **b** the contact networks of both communities obey a Poisson distribution
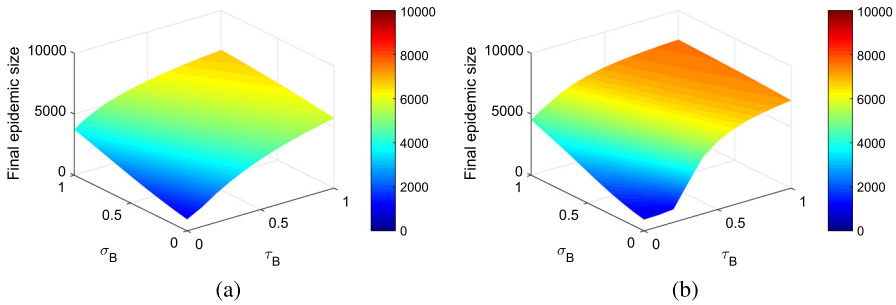
Fig. 14 The relation of the final size (i.e. the number of individuals affected by disease) to τ_B (disease transmission probability within community B) and σ_B (disease transmission probability from community A to community B): **a** the contact networks of both communities obey a Power-law distribution; **b** the contact networks of both communities obey a Poisson distribution

networks of both communities obey the Power-law distribution when the parameters are all the same.

5 Concluding remarks

Communities are often interconnected and exhibit asymmetric interactions among them. The infectious disease can therefore be transmitted in a population through both network contacts within communities and casual contacts between different communities (Diekmann et al. 1998; Ball and Neal 2002). Previous research based on the homogeneous population mixing assumption may not accommodate such epidemic transmission considerations. Motivated by the fact that the epidemic may be affected by both intra-community and inter-community transmissions, we have formulated a two-community SIR epidemic model with asymmetric coupling. For this two-community SIR model with asymmetric coupling, we utilized an edge-based compartmental modeling approach to derive a low-dimensional model corresponding to the original model. This enabled us to attain an explicit expression for the basic
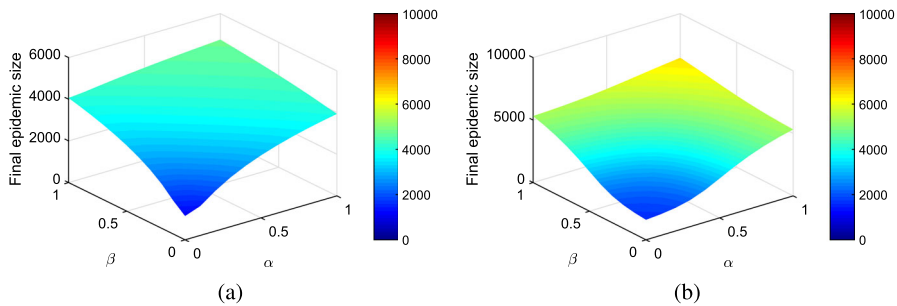
Fig. 15 The relation of the final size (i.e. the number of individuals affected by disease) to α (the contribution of disease transmission within community A) and β (the contribution of disease transmission within community B): **a** the contact networks of both communities obey a Power-law distribution; **b** the contact networks of both communities obey a Poisson distribution

reproduction number, which intriguingly manifests as a root of a quaternion equation. Additionally, we derived an implicit equation for the final size and demonstrated the existence and uniqueness of its solution through the construction of appropriate mappings. Based on these theoretical results, we investigated the effects of contact heterogeneity and asymmetric coupling on the basic reproduction number, final size, and their relationship. This proposed model, along with these analyses, will contribute to a deeper understanding of transmission mechanisms underlying infectious diseases in large populations, allowing more efficient community-based preventive measures and aiding in mitigation measures.

The findings presented in this paper demonstrate that incorporating contact heterogeneity and asymmetric coupling between communities in an epidemic model can yield results that differ from those based on a single homogeneously mixed population model. This discrepancy is particularly evident when considering the two crucial quantities: the basic reproduction number ($\mathcal{R}_0$) and the final epidemic size (z). An intriguing finding of our study is the relationship between $\mathcal{R}_0$ and z. In the classical SIR model, $\mathcal{R}_0$ and z display a positive correlation, as demonstrated in Fig. 5. However, when considering contact heterogeneity and asymmetric coupling between the two communities in the model, this relationship may be reversed, as depicted in Fig. 6. Specifically, we found that an increase in the difference between the number of individual contacts k_1 and k_2 within the community leads to an increase in $\mathcal{R}_0$ and a decrease in z. The result of an increase in $\mathcal{R}_0$ in this case is consistent with the previous study by Tilman and Kareiva (1998), which suggested that $\mathcal{R}_0$ tends to be greater in the presence of salient spatial or heterogeneous characteristics. Counterintuitively, mitigation efforts on reducing the outbreak crises (i.e. $\mathcal{R}_0$) may not necessarily result in a lower number of individuals eventually affected by disease (i.e. z) when including interactions between communities. Hence, solely relying on $\mathcal{R}_0$ or z to formulate prevention policies may be misleading.

Another interesting finding of our study is that limiting the movement of susceptible individuals in a community has a complex effect on $\mathcal{R}_0$, where $\mathcal{R}_0$ does not follow a simple monotonous relationship, as illustrated in Fig. 2. We further present a more comprehensive model (3.28) that not only reproduces the result that restricting the

movement of susceptible individuals in a community makes $\tilde{R}_0$ non-monotonous but also uncovers the relationship where $\tilde{R}_0$ is an increasing function of both $\tilde{\alpha}$ and $\tilde{\beta}$. This suggests that restricting the movement of susceptible individuals solely within a community may not be an effective measure for controlling the disease, and additional factors should be considered when developing prevention strategies. Additionally, our results showed that network contacts within communities have a greater effect on the basic reproduction number than casual contacts between communities. The basic reproduction number is greater under a Power-law distribution than under a Poisson distribution (cf. Fig. 7), while the opposite observation appears in the final size of the disease (cf. Fig. 13).

This paper only considers a two-community epidemic model without demographics. Expanding the model to include demographics of n communities allows for the inclusion of more complex dynamics. Further discussion on the epidemic peak and the time reaching the peak (Cadoni 2020; Turkyilmazoglu 2021) remains to be done, since the epidemic peak reflects the severity of an infectious disease and can provide a scientific basis for the health department's planning of limited medical resources. In addition, nested models linking within-host viral dynamics and between-host disease transmission dynamics are currently receiving a lot of attention from researchers, and take into account the importance of spatial heterogeneity factors and the infection age in studying epidemic transmission models. We subsequently intend to investigate some of the dynamics of age-spatial nested models, such as the final size, using the approaches in Thieme (1977) and Diekmann (1978). The uniqueness of the solution to the final size equation may be able to be proved along the lines of Thieme (1979) using the sublinearity/subhomogenity/concavity method for uniqueness in Krasnosel'skii (1964), Sec. 6.1. We will examine this in detail in our future work.

Appendix

We can obtain the roots of the quaternion equation (3.10) using the Ferrari's solution (see, https://en.wikipedia.org/wiki/Quartic_function#Ferraris_solution for the exact solution procedure):

$$\lambda_1 = \frac{\rho_{lA} + \rho_{lB}}{4} + \frac{\sqrt{\mu + 2y} + \sqrt{-(3\mu + 2y + \frac{2v}{\sqrt{\mu+2y}})}}{2},$$

$$\lambda_2 = \frac{\rho_{lA} + \rho_{lB}}{4} + \frac{\sqrt{\mu + 2y} - \sqrt{-(3\mu + 2y + \frac{2v}{\sqrt{\mu+2y}})}}{2},$$

$$\lambda_3 = \frac{\rho_{lA} + \rho_{lB}}{4} - \frac{\sqrt{\mu + 2y} + \sqrt{-(3\mu + 2y - \frac{2v}{\sqrt{\mu+2y}})}}{2},$$

$$\lambda_4 = \frac{\rho_{lA} + \rho_{lB}}{4} - \frac{\sqrt{\mu + 2y} - \sqrt{-(3\mu + 2y - \frac{2v}{\sqrt{\mu+2y}})}}{2},$$

where

$$\mu = \frac{1}{8}(-3\rho_{lA}^2 + 2\rho_{lA}\rho_{lB} - 3\rho_{lB}^2 - 8\rho_{gA}\rho_{gB}),$$

$$v = -\frac{\rho_{lA}\rho_{gA}\rho_{gB}(2\langle k\rangle_A^2 - \langle k^2\rangle_A)}{2\langle k^2\rangle_A} - \frac{\rho_{lA}^3 - \rho_{lA}^2\rho_{lB} - \rho_{lA}\rho_{lB}^2 + \rho_{lB}^3}{8}$$
$$+ \frac{\rho_{lB}\rho_{gA}\rho_{gB}(\langle k^2\rangle_B - 2\langle k\rangle_B^2)}{2\langle k^2\rangle_B},$$

$$\upsilon = -\frac{\rho_{lA}^2\rho_{gA}\rho_{gB}}{16\langle k^2\rangle_A}\left(4\langle k\rangle_A^2 - 3\langle k^2\rangle_A\right) - \frac{\rho_{lA}\rho_{lB}\rho_{gA}\rho_{gB}}{8\langle k^2\rangle_A\langle k^2\rangle_B}\left(5\langle k^2\rangle_A\langle k^2\rangle_B - 6\langle k\rangle_A^2\langle k^2\rangle_B\right.$$
$$\left. - 6\langle k^2\rangle_A\langle k\rangle_B^2 + 8\langle k\rangle_A^2\langle k\rangle_B^2\right) + \frac{1}{256}\left(4\rho_{lA}^3\rho_{lB} + 4\rho_{lA}\rho_{lB}^3 - 3\rho_{lA}^4 + 14\rho_{lA}^2\rho_{lB}^2 - 3\rho_{lB}^4\right)$$
$$+ \frac{\rho_{lB}^2\rho_{gA}\rho_{gB}}{16\langle k^2\rangle_B}\left(3\langle k^2\rangle_B - 4\langle k\rangle_B^2\right),$$

$$y = -\frac{5}{6}\mu - \frac{P}{3U} + U, \quad P = -\frac{\mu^2}{12} - \upsilon, \quad Q = -\frac{\mu^3}{108} + \frac{\mu\upsilon}{3} - \frac{v^2}{8},$$

$$U = \sqrt[3]{-\frac{Q}{2} \pm \sqrt{\frac{Q^2}{4} + \frac{P^3}{27}}} \text{(take the value with the larger mode).}$$

References

Amini H, Minca A (2022) Epidemic spreading and equilibrium social distancing in heterogeneous networks. Dyn Games Appl 1–30

Anderson RM, May RM (1992) Infectious diseases of humans: dynamics and control. Oxford University Press, Oxford

Ball F, Neal P (2002) A general model for stochastic SIR epidemics with two levels of mixing. Math Biosci 180(1–2):73–102

Barthélemy M, Barrat A, Pastor-Satorras R et al (2005) Dynamical patterns of epidemic outbreaks in complex heterogeneous networks. J Theor Biol 235(2):275–288

Bidari S, Chen X, Peters D et al (2016) Solvability of implicit final size equations for SIR epidemic models. Math Biosci 282:181–190

Cadoni M (2020) How to reduce epidemic peaks keeping under control the time-span of the epidemic. Chaos Solitons Fractals 138:109940

Cui J, Wu Y, Guo S (2022) Effect of non-homogeneous mixing and asymptomatic individuals on final epidemic size and basic reproduction number in a meta-population model. Bull Math Biol 84(3):1–22

Diekmann O (1978) Thresholds and travelling waves for the geographical spread of infection. J Math Biol 6(2):109–130

Diekmann O, De Jong MCM, Metz JAJ (1998) A deterministic epidemic model taking account of repeated contacts between the same individuals. J Appl Probab 35(2):448–462

El Sayed NM, Gomatos PJ, Beck-Sagué CM et al (2000) Epidemic transmission of human immunodeficiency virus in renal dialysis centers in Egypt. J Infect Dis 181(1):91–97

Ferrari's solution. https://en.wikipedia.org/wiki/Quartic_function#Ferraris_solution

Fitzgibbon WE, Morgan JJ, Webb GF et al (2019) Spatial models of vector-host epidemics with directed movement of vectors over long distances. Math Biosci 312:77–87

Fitzgibbon WE, Morgan JJ, Webb GF et al (2020) Analysis of a reaction-diffusion epidemic model with asymptomatic transmission. J Biol Syst 28(03):561–587

Graham M, House T (2014) Dynamics of stochastic epidemics on heterogeneous networks. J Math Biol 68(7):1583–1605

Großmann G, Backenköhler M, Wolf V (2021) Heterogeneity matters: contact structure and individual variation shape epidemic dynamics. PLoS ONE 16(7):e0250050

Hales S, Weinstein P, Souares Y et al (1999) El Niño and the dynamics of vectorborne disease transmission. Environ Health Perspect 107(2):99–102

Hethcote HW (2000) The mathematics of infectious diseases. SIAM Rev 42(4):599–653

Jin Z, Sun G, Zhu H (2014) Epidemic models for complex networks with demographics. Math Biosci Eng 11(6):1295

Kamp C (2010) Untangling the interplay between epidemic spread and transmission network dynamics. PLoS Comput Biol 6(11):e1000984

Kiss IZ, Green DM, Kao RR (2006) The effect of contact heterogeneity and multiple routes of transmission on final epidemic size. Math Biosci 203(1):124–136

Koch D, Illner R, Ma J (2013) Edge removal in random contact networks and the basic reproduction number. J Math Biol 67(2):217–238

Krasnosel'skii MA (1964) Positive solutions of operator equations. Nordhoff, Groningen

Lajmanovich A, Yorke JA (1976) A deterministic model for gonorrhea in a nonhomogeneous population. Math Biosci 28(3–4):221–236

Li CH, Tsai CC, Yang SY (2014) Analysis of epidemic spreading of an SIRS model in complex heterogeneous networks. Commun Nonlinear Sci Numer Simul 19(4):1042–1054

Lieberthal B, Soliman A, Wang S et al (2023) Epidemic spread on patch networks with community structure. Math Biosci 359:108996

Magal P, Seydi O, Webb GF (2016) Final size of an epidemic for a two-group SIR model. SIAM J Appl Math 76(5):2042–2059

Magal P, Seydi O, Webb GF (2018) Final size of a multi-group SIR epidemic model: irreducible and non-irreducible modes of transmission. Math Biosci 301:59–67

Meng X, Cai Z, Si S et al (2021) Analysis of epidemic vaccination strategies on heterogeneous networks: based on SEIRV model and evolutionary game. Appl Math Comput 403:126172

Miller JC, Slim AC, Volz EM (2012) Edge-based compartmental modelling for infectious disease spread. J R Soc Interface 9(70):890–906

Moreno Y, Pastor-Satorras R, Vespignani A (2002) Epidemic outbreaks in complex heterogeneous networks. Eur Phys J B Condens Matter Complex Syst 26(4):521–529

Mossong J, Hens N, Jit M et al (2008) Social contacts and mixing patterns relevant to the spread of infectious diseases. PLoS Med 5(3):e74

Muroya Y, Kuniya T (2014) Further stability analysis for a multi-group SIRS epidemic model with varying total population size. Appl Math Lett 38:73–78

Muroya Y, Enatsu Y, Kuniya T (2013) Global stability for a multi-group SIRS epidemic model with varying population sizes. Nonlinear Anal Real World Appl 14(3):1693–1704

Olinky R, Stone L (2004) Unexpected epidemic thresholds in heterogeneous networks: the role of disease transmission. Phys Rev E 70(3):030902

Pastor-Satorras R, Vespignani A (2001) Epidemic dynamics and endemic states in complex networks. Phys Rev E 63(6):066117

Rass L, Radcliffe J (2003) Spatial deterministic epidemics. American Mathematical Society

Thieme HR (1977) A model for the spatial spread of an epidemic. J Math Biol 4:337–351

Thieme HR (1979) On a class of Hammerstein integral equations. Manuscr Math 29:49–84

Thieme HR (2003) Mathematics in population biology. Princeton University Press, Princeton

Tilman D, Kareiva P (1998) Spatial ecology. Princeton University Press, Princeton

Turkyilmazoglu M (2021) Explicit formulae for the peak time of an epidemic from the SIR model. Phys D 422:132902

Van den Driessche P, Watmough J (2002) Reproduction numbers and sub-threshold endemic equilibria for compartmental models of disease transmission. Math Biosci 180(1–2):29–48

Velazquez O, Stetler HC, Avila C et al (1990) Epidemic transmission of enterically transmitted non-A, non-B hepatitis in Mexico, 1986–1987. JAMA 263(24):3281–3285

Wallis J, Lee DR (1999) Primate conservation: the prevention of disease transmission. Int J Primatol 20(6):803–826

Wang L, Dai G (2008) Global stability of virus spreading in complex heterogeneous networks. SIAM J Appl Math 68(5):1495–1502

Wang Y, Jin Z, Yang Z et al (2012) Global analysis of an SIS model with an infective vector on complex networks. Nonlinear Anal Real World Appl 13(2):543–557

Wang Y, Cao J, Li X et al (2018) Edge-based epidemic dynamics with multiple routes of transmission on random networks. Nonlinear Dyn 91(1):403–420

Wang Y, Wei Z, Cao J (2020) Epidemic dynamics of influenza-like diseases spreading in complex networks. Nonlinear Dyn 101(3):1801–1820

Yorke JA (1967) Invariance for ordinary differential equations. Math Syst Theory 1(4):353–372

Zhang J, Jin Z (2012) Epidemic spreading on complex networks with community structure. Appl Math Comput 219(6):2829–2838

Zhu G, Fu X, Chen G (2012) Spreading dynamics and global stability of a generalized epidemic model on complex heterogeneous networks. Appl Math Model 36(12):5808–5817